Title

Electrodes modified with molecular catalysts for the electrochemical reduction of CO2 to CO

Permalink

https://escholarship.org/uc/item/6j41r88x

Author

Zhanaidarova, Almagul

Publication Date

2019

Peer reviewed|Thesis/dissertation

UNIVERSITY OF CALIFORNIA SAN DIEGO

Electrodes modified with molecular catalysts for the electrochemical reduction of CO_2 to CO

A dissertation submitted in partial satisfaction of the requirements for the degree

Doctor of Philosophy

in

Materials Science and Engineering

by

Almagul Zhanaidarova

Committee in charge:

Professor Clifford P. Kubiak, Chair
Professor Prabhakar Bandaru
Professor Michael Gilson
Professor Jeffrey Rinehart
Professor Valerie Schmidt
Professor Wei Xiong

2019

All rights reserved. The dissertation of Almagul Zhanaidarova is approved, and it is acceptable in quality and form for publication on microfilm and electronically:

Chair

University of California, San Diego

2019

DEDICATION

This dissertation is dedicated to my family, my friends and my cats.

TABLE OF CONTENTS

LIST OF FIGURES

LIST OF SCHEMES

LIST OF TABLES

AKNOWLEDGEMENTS

I would like to thank my parents for giving me love and support, for teaching me respect and appreciation, for encouraging me to be creative and follow my own path in life. Thank you for teaching me values that I'm carrying throughout my life even thousand miles away from you. I want to thank my spouse Eldar for moral and material support throughout my graduate studies. Thanks to my older sister Mira for all her support and wisdom. I would like to thank Professor Kubiak and his wife Pam for making UCSD my home for 6 years of my graduate studies. Thanks to Cliff for his support and opportunities that he gave me, especially for giving me the research freedom and allowing me to establish myself as a scientist. I would like to thank our collaborators at the Electrochemical Technologies Group at JPL/NASA and especially Dr. Simon Jones, for his patience and efforts to make our collaboration possible and for giving me the freedom and allowing me to develop my scientific skills and apply my knowledge to practice. For making me feel valued and appreciated. I would like to give a special acknowledgment to Professor Harry B. Gray at Caltech. Harry let me to join his lab when I first came to the US and forever changed my perspective on inorganic chemistry and materials science. His support and the greatness of his character inspired me for all the discoveries that came ahead. I'm grateful to Professor Qixi Mi, who was a postdoc and my supervisor during my years at Caltech for all his patience and shared knowledge. I would like to specially thank Professor Hemamala Karunadasa at Stanford University. I learned so much from Hema, she was a true mentor for me, teaching me chemistry and all the lab skills that I carried throughout my days at Stanford and that I have been constantly using since then. I would like to thank all my Stanford and Caltech friends, especially Dr. Nicole Bouley-Ford for all her support and influence in the beginning of my time at Caltech.

I would like to thank all my UCSD friends for all their support and for sharing the graduate school experience with me. I would like to thank my friends from my home country Kazakhstan, and especially those who are similar to me, pursuing their graduate studies in the US, with whom we established the special bond that I hope to carry throughout my life.

CHAPTER SPECIFIC ACKNOWLEDGEMENTS

Chapter 2. The material for Chapter 2 comes directly from manuscript entitled " Re(tBu-bpy)$(CO)_3Cl$ supported on multi-walled carbon nanotubes selectively reduces CO_2 in water. " by Almagul Zhanaidarova, Brian Pimentel, Simon C. Jones and Clifford P. Kubiak, which is currently in preparation. The dissertation author is the primary author of this paper.

Chapter 3. The material for Chapter 3 comes directly from manuscript entitled "Selective Reduction of CO_2 to CO by a Molecular Re(ethynyl-bpy)$(CO)_3Cl$ atalyst and Attachment to Carbon Electrode Surfaces" by Almagul Zhanaidarova, Andrew L. Ostericher, Christopher J. Miller, Simon C. Jones and Clifford P. Kubiak, which has been published in the Journal of *Organometallics*, **2019**, *38* (6), pp 1204. The dissertation author is the primary author of this paper.

Chapter 4. The material for Chapter 4 comes directly from manuscript entitled "Covalent attachment of $[Ni(alkynyl\text{-}cyclam)]^{2+}$ catalysts to glassy carbon electrodes" by Almagul Zhanaidarova, Curtis E. Moore, Milan Gembicky and Clifford P. Kubiak, which has been published in the *Chemical Communications* **2018**, *54*, 4116. The dissertation author is the primary author of this paper.

VITA

2013-2019	University of California San Diego. Doctor of Philosophy. PI: Professor Clifford Kubiak
2012 - 2013	Stanford University. Research Assistant. PI: Professor Hemamala Karunadasa
2010 - 2012	California Institute of Technology. Research Assistant. PI: Professor Harry B. Gray
2007 - 2008	Alex Stewart Geo Analytical Lab. Laboratory Assistant. Moscow, Russia
2007	Mendeleev University of Chemical Technology of Russia. Master of Science
2005	Mendeleev University of Chemical Technology of Russia. Bachelor of Science

PATENTS

1. U.S. Provisional Application 62/827, 597, SD2019-283: "Electrochemical conversion" - 2019.

PUBLICATIONS

1. Re(tBu-bpy)$(CO)_3Cl$ supported on multi-walled carbon nanotubes selectively reduces CO_2 in water. Zhanaidarova A., Pimentel B., Jones S. C., Kubiak C. P., **2019**. *Manuscript in preparation.*

2. Selective reduction of CO_2 to CO by a molecular Re(ethynyl-bpy)$(CO)_3Cl$ catalyst and attachment to carbon electrode surfaces. Zhanaidarova A., Ostericher A. L., Miller C. J., Jones S. C., Kubiak C. P., *Organometallics*, **2019**, *38* (6), pp 1204–1207

3. Covalent attachment of $[Ni(alkynyl\text{-}cyclam)]^{2+}$ catalysts to glassy carbon electrodes. Zhanaidarova A., Moore C. E., Gembicky M., Kubiak C. P., *Chem. Commun.*, **2018,** *54*, 4116 – 4119.

4. Chelated $[Zn(cyclam)]^{2+}$ Lewis acid improves the reactivity of the electrochemical reduction of CO 2 by Mn catalysts with bulky bipyridine ligands. Zhanaidarova A., Steger H., Reineke M. H., Kubiak C.P., *Dalton Trans.*, **2017**, *46,* 12413-12416.

5. Electrode-ligand interactions dramatically enhance CO_2 conversion to CO by the [Ni(cyclam)]$(PF_6)_2$ catalyst. Wu Y., Rudshtein B., Zhanaidarova A., Froehlich J. D., Ding W., Kubiak C. P., Batista V. S., *ACS Catal.* **2017,** *7* (8), 5282 -5288.

6. A quantitative assessment of the competition between water and anion oxidation at WO_3 photoanodes in acidic aqueous electrolytes. Mi Q., Zhanaidarova A., Brunschwig B. S., Gray H. B., Lewis N. S., *Energy Environ. Sci.,* **2012,** *5*, 5694-5700.

ABSTRACT OF THE DISSERTATION

Electrodes modified with molecular catalysts for the electrochemical reduction of CO_2 to CO

by

Almagul Zhanaidarova

Doctor of Philosophy in Materials Science and Engineering

University of California San Diego, 2019

Professor Clifford P. Kubiak, Chair

Our current energy needs depend mostly on non-sustainable fuels: coal, oil and natural gas. Carbon dioxide that comes from fossil fuels accounts for 65% of greenhouse gas emission that plays a major role in climate change. Therefore, the development of an alternative carbon cycle that includes production of sustainable fuels should be the priority for the future of our planet. The electrochemical CO_2 reduction to CO and further utilization of CO to fuels and chemicals is a promising pathway from both economic and environmental points of view. The main challenge to implement this technology at an industrial scale is to find the catalyst that will be robust, selective and sustain high conversion efficiency. This thesis describes approaches to solving this problem. One of the most effective electrocatalytic systems for the electrochemical reduction of CO_2 to CO was described in Chapter 2 of this thesis, where $Re(tBu\text{-}bpy)(CO)_3Cl$ molecular catalyst was incorporated into the structure of MWCNTs and new heterogeneous material was developed. This material obtained all advantages of both homogeneous and heterogeneous catalysts. This system is considered to be one of the most selective and robust among other developed CO_2 electroreduction systems by present day. The developed

heterogeneous materials can find its application not only on the planet Earth but has a potential to be used in the future interstellar missions.

The development of Re(tBu-bpy)$(CO)_3Cl$/MWCNT heterogeneous material was carried out under the support of NASA/JPL as an alternative for the current technology that is being tested on a planet Mars, where CO_2 gas represents 90-95% of the Martian atmosphere. The Mars Oxygen In-Situ Resource Utilization Experiment is better known as MOXIE reduces CO_2 to CO and produces Oxygen gas that is vital for supporting human life during the interstellar missions. This device utilizes yttria-stabilized zirconia and operates at 700°C. Thus, the development of an alternative electrochemical device that operates at room temperature is of a great interest and a serious challenge. Chapter 2 of this thesis describes the main breakthrough in the development of a key part of such a device - the cathode at which selective CO_2 reduction to CO occurs. The development of a complete device that reduces CO_2 to CO at the cathode and produces O_2 gas at the anode stands among future challenges and is a subject of a future research.

Chapter 1

1.1 Electrochemical reduction of CO_2

The electrochemical reduction of carbon dioxide, combined with renewable sources of energy such as wind or solar, can be a promising pathway to convert CO_2 to valuable fuels and chemicals.

The availability of solar-generated electricity in some regions can exceed demand during daylight hours.[1] Advanced energy storage technologies are required to bank excess capacity for use during peak demand periods later in the day. One potential use of excess renewable electricity is the electrochemical production of fuels and chemicals.[2] The development of robust and efficient systems for electrochemical CO_2 reduction to CO is a promising approach to the conversion of CO_2 to valuable products. This is a promising pathway to help mitigate climate change while contributing to the world's energy supply. The electrochemical reduction of CO_2 to CO with renewable electricity provides a green path to synthesis gas and thereby a wide variety of chemicals and fuels via the Fisher-Tropsch process.[3]

Originally developed in early 1920s, Fisher-Tropsch process is a series of chemical reactions involved the conversion of carbon monoxide and hydrogen into liquid fuels according to Equation 1.1:

$$(2n + 1)H_2 + nCO \rightarrow C_nH_{2n+2} + nH_2O \qquad \text{Eq. 1.1}$$

Where for n=1, the reaction represents production of methane, and for n>1 reaction represents production of higher hydrocarbons. It is important to choose the optimal conditions for the production of liquid fuels, as the water-gas-shift reactions may occur, where hydrogen gas and carbon dioxide are main products, according to Eg. 1.2:

$CO + H_2O \rightarrow H_2 + CO_2$ Eq. 1.2

Various hydrocarbons from methane to olefins and paraffin can be obtained through Fisher-Tropsch reactions, based on the chosen temperature, pressure and catalyst, according to Figure 1.1:

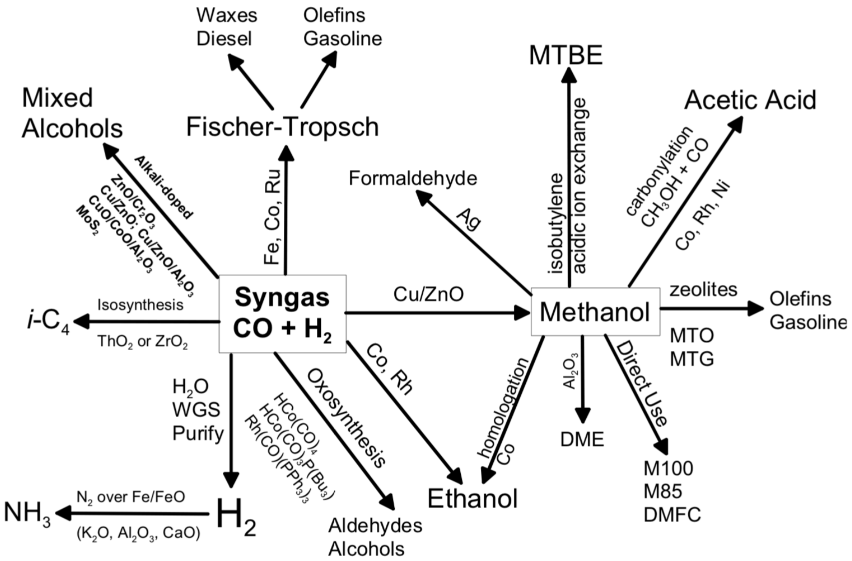

Figure 1.1 Schematic representation of synthesis gas conversion.[4]

The current technological pathway to produce CO, the main feedstock for the Fisher-Tropsch process, derived from coal and natural gas. Purification of the syngas feedstock estimates for 60-70 % of the total cost of the end product. Production of pure carbon monoxide is of a great interest, because it can significantly decrease the overall cost of the Fisher-Tropsch technology.

Efficient electrochemical CO_2 reduction to CO will not only contribute to the purity of the feedstock carbon monoxide but can potentially decrease the overall concentration of the CO_2 gas in the atmosphere.

1.2 Thermodynamic considerations

Electrochemical CO_2 reduction to various products can occur in accordance with their thermodynamic potentials following Equation 1.3 -1.8 (pH 7 in aqueous solution versus a normal hydrogen electrode (NHE), 25◦C, 1 atm gas pressure)[5]:

$$CO_2 + 2H^+ + 2e^- \rightarrow CO + H_2O \qquad E^{\circ} = -0.53\ V \qquad \text{Eq. 1.3}$$

$$CO_2 + 2H^+ + 2e^- \rightarrow HCO_2H \qquad E^{\circ} = -0.61\ V \qquad \text{Eq. 1.4}$$

$$CO_2 + 4H^+ + 4e^- \rightarrow HCHO + H_2O \qquad E^{\circ} =-0.48\ V \qquad \text{Eq. 1.5}$$

$$CO_2 + 6H^+ + 6e^- \rightarrow CH_3OH + H_2O \qquad E^{\circ} = -0.38\ V \qquad \text{Eq. 1.6}$$

$$CO_2 + 8H^+ + 8e^- \rightarrow CH_4 + 2H_2O \qquad E^{\circ} = -0.24\ V \qquad \text{Eq. 1.7}$$

$$CO_2 + e^- \rightarrow CO2^{\bullet -} \qquad E^{\circ} = -1.9\ V \qquad \text{Eq.1 8}$$

Considerable kinetic challenges should also be taken into account for the production of products involving multiple electron and proton transfer reactions (PCET), as these reactions usually associated with high activation energies presenting significant kinetic barriers. Thus, production of higher hydrocarbons, through electrochemical CO_2 reduction, such as methanol and formic acid, have only been reported with relatively low efficiency. On the other hand, efficient electrochemical reduction of CO_2 to CO was achieved with a number of molecular catalysts.[6]

1.3 Homogeneous and heterogeneous electrocatalysts:

The two main classes of catalysts are described in this chapter: homogeneous and heterogeneous and a motivation to combine these two classes of catalysts in one hybrid system.

Homogeneous electrocatalysts are catalysts dissolved in electrolyte solution and are able to freely diffuse to the surface of the electrode. The substrate tent to be dissolved in solution as well. The efficiency of the homogeneous electroreduction usually determined by the thermodynamic potential as well as the diffusion of the catalyst and substrate to the surface of the electrode. There are various homogeneous electrocatalysts that can efficiently reduce CO_2 to CO.[5, 6]

The heterogeneous catalysis describes the system where the active catalyst represents the bulk solid electrode material, usually metal electrodes or surface modified electrodes. In this case only the substrate must diffuse to the electrode surface and the efficiency of the reaction will be determined by the diffusion of the substrate and overall thermodynamic limitations.

The properties of various metal electrodes for the electrochemical reduction of CO_2 was previously described by Hori et al., and led to the development of a variety of metallic electrodes for CO_2 reduction to CO, methane and even C_2 – C_3 organic species.[7] Metal nanoparticle electrocatalysts composed of Ag[8] and Au[9] have been reported to operate in aqueous solutions at low overpotentials.[9, 10] The recent development of nanostructured copper based electrodes led to the production of C1 - C3 organic species depending on the conditions and active sites of metallic copper.[11, 12] These nanostructured electrodes can be complicated to prepare, and often require additional etching steps and expensive equipment. In operation, they can suffer from oxidation processes, and surface reconstruction that decrease selectivity and longevity.

Modification of electrode surfaces with molecular catalysts is a promising path towards development of robust, selective and efficient heterogeneous materials for the electrochemical CO_2 reduction. Employing catalysts on support materials can also significantly reduce catalyst loadings and overall cost. Studies of molecular catalysts on a variety of conducting materials have been reported recently.[13-17] Molecular catalysts can combine high selectivity and reactivity towards CO_2 reduction, and these can be varied via control of structural and electronic properties.

The homogeneous catalysts of two families will be mainly covered in this thesis: fac-Re(4,4’-R-2,2′-bipyridine)$(CO)_3X$ and $[Ni(R\text{-cyclam})]^{2+}$. Attempts to heterogenized these catalysts will be covered in Chapter 2 and Chapter 3 and Chapter 4.

1.4 References

1. Denholm P.; O'Connell M.; Brinkman G.; Jorgenson J., Overgeneration from Solar Energy in California: A Field Guide to the Duck Chart. *National Renewable Energy Laboratory*, **2015**.

2. Lewis N. S.; Nocera D. G., Powering the planet: Chemical challenges in solar energy utilization. *PNAS*, **2006**. *103*(43): p. 15729-15735.

3. Steynberg A. P., Introduction to Fihser-Tropsch Technology. *Studies in Surface Science and Catalysis*, **2004**. *152*: p. 1-63.

4. Spath P. L.; Dayton D. C., Preliminary Screening — Technical and Economic Assessment of Synthesis Gas to Fuels and Chemicals with Emphasis on the Potential for Biomass-Derived Syngas; NREL/TP-510-34929. *National Renewable Energy Laboratory: Golden, VA*, **2003**.

5. Benson E. E.; Kubiak C. P.; Sathrum A. J.; Smieja J. M., Electrocatalytic and homogeneous approaches to conversion of CO2 to liquid fuels. *Chem. Soc. Rev.*, **2009**. *38*(1): p. 89-99.

6. Francke R.; Schille B.; Roemelt M., Homogeneously Catalyzed Electroreduction of Carbon Dioxide: Methods, Mechanisms, and Catalysts. *Chem. Rev.*, **2018**. *118*: p. 4631-4701.

7. Hori Y. K.; Suzuki S., Production of CO and CH4 in Electrochemical Reduction of CO2 at Metal Electrodes in Aqueous Hydrogencarbonate Solution. *Chem. Lett.*, **1985**. *14*: p. 1695-1698.

8. Lu Q.; Rosen J.; Zhou Y.; Hutchings G. S.; Kimmel Y. C.; Chen J. G.; Jiao F., A Selective and Efficient Electrocatalyst for Carbon Dioxide Reduction. *Nat. Commun.*, **2014**. *5*: p. 3242.

9. Chen Y.; Li C. W.; Kanan M. W., Aqueous CO2 Reduction at Very Low Overpotential on Oxide-Derived Au Nanoparticles. *J. Am. Chem. Soc.*, **2012**. *134*: p. 19969-19972.

10. Welch A. J.; DuChene J. S.; Tagliabue G.; Davoyan A.; Cheng W. H.; Atwater H. A., Nanoporous Gold as a Highly Selective and Active Carbon Dioxide Reduction Catalyst. *Appl. Energy Mater.*, **2019**. *2*(1): p. 164-170.

11. Li C. W.; Kanan M. W., CO2 Reduction at Low Overpotential on Cu Electrodes Resulting from the Reduction of Thick Cu2O Films. *J. Am. Chem. Soc.*, **2012**. *134*(17): p. 7231-7234.

12. Zhou X.; Micheroni D.; Lin Z.; Poon C.; Li Z.; Lin W., Graphene-Immobilized fac-Re(bipy)(CO)3Cl for Syngas Generation from Carbon Dioxide. *ACS Appl. Mater. Interfaces*, **2016**. *8*(6): p. 4192-4198.

13. Zhanaidarova A.; Moore C.E.; Gembicky M.; Kubiak C. P., Covalent Attachment of [Ni(alkynyl-cyclam)]2+ Catalysts to Glassy Carbon Electrodes. *Chem. Commun*, **2018**. *54*(4116-4119).

14. Tran P. D.; Le Goff A.; Heidkamp J.; Jousselme B.; Guillet N.; Palacin S.; Dau H.; Fontecave M.; Artero V., Noncovalent Modification of Carbon Nanotubes with Pyrene-Functionalized Nickel Complexes: Carbon Monoxide Tolerant Catalysts for Hydrogen Evolution and Uptake. *Angew. Chem. Int. Ed. Engl*, **2011**. *50*(6): p. 1371.

15. Sun C.; Rotundo L.; Garino C.; Nencini L.; Yoon S. S.; Gobetto R.; Nervi C., Electrochemical CO2 Reduction at Glassy Carbon Electrodes Functionalized by MnI and ReI Organometallic Complexes. *ChemPhysChem*, **2017**. *18*: p. 3219.

16. Neri G., W.J.J., Wilson G., Reynal A., Lim J. Y. C., Li X., White A. J. P., Long N. J., Durrant J. R., Cowan A.,, A Functionalised Nickel Cyclam Catalyst for CO2 Reduction: Electrocatalysis, Semiconductor Surface Immobilisation and Light-Driven Electron Transfer. *Phys. Chem. Chem. Phys.*, **2015**. *17*: p. 1562-1566.

17. Jackson M. N.; Oh S.; Kaminsky C. J.; Chu S. B.; Zhang G.; Miller J. T.; Surendranath Y., Strong Electronic Coupling of Molecular Sites to Graphitic Electrodes via Pyrazine Conjugation. *J. Am. Chem. Soc.*, **2018**. *140*(3): p. 1004-1010.

Chapter 2

Re(tBu-bpy) supported by MWCNT

2.1 Introduction

This chapter will focus on the modification of a carbon electrodes with Re(tBu-bpy) electrocatalyst. The incorporation of molecular catalysts into the structure of carbon nanotubes provides a promising strategy for the development of hybrid molecular/heterogeneous catalyst materials that retain the desirable properties of molecular catalysts, particularly selectivity. Multi-walled carbon nanotubes (MWCNT) represent a very interesting electrode material for catalyst incorporation into a high surface area matrix with excellent electrical conductivity.[1] A number of reports describe surface modified carbon nanotubes with molecular catalysts.[2-5] The recently reported hybrid CoPc/carbon nanotube structures provided high current densities, high turnover frequency and good selectivity towards CO_2 reduction to CO ($FE_{CO} > 95\%$) in neutral aqueous media at low overpotential (0.52 V).[6] Manganese catalysts polymerized at the surface of MWCNT/CNF (carbon nanofiber) also performed as efficient catalytic systems for electrochemical reduction of CO_2 to CO, operating at low potential (-0.39 V vs. RHE) in $K_2B_4O_7$ + K_2SO_4 aqueous solution.[7]

The catalysts of the family fac-Re(4,4'-R-2,2′-bipyridine)$(CO)_3X$ (where R varies from electron- withdrawing to electron-donating substituents, and X = Cl, Br, CH_3CN, CH_3CN(Otf), Py(OTf), etc.) with the Re(R-bpy) motif are well known for their electrochemical and photosensitized reactivity towards CO_2 reduction.[8] Reports of incorporation into higher-order polymeric systems[9, 10] and surface attachment[11, 12] of these catalysts illustrate their versatility.[13] One of the most efficient and durable catalysts of this class is Re(4,4'-tBu-2,2'-bpy)$(CO)_3$Cl, known for its ability to convert CO_2 to CO with 100% Faradaic efficiency (FE) in organic media.[14]

Re(4,4'-tBu-2,2'-bpy)$(CO)_3$Cl was incorporated into MWCNTs for the first time. Confined into the bulk structure of MWCNTs the Re(tBu-bpy) catalyst performs as a superior catalyst for CO_2 reduction in every measurable figure of merit, compared to the homogeneous molecular catalyst: Faradaic efficiency for CO FE_{CO} = 99% and less than 1% H_2, low operating potential (-0.56 V vs. RHE), able to sustain constant CO production for more than 7 h, and it works in water with 0.5 M $KHCO_3$ supporting electrolyte.

The Re(tBu-bpy)$(CO)_3$Cl catalyst has been widely studied as a homogeneous catalyst in organic solvents Re(tBu-bpy)$(CO)_3$Cl. In contrast to organic solvents, the highly selective electrochemical reduction of CO_2 to CO in water by a Re(tBu-bpy)$(CO)_3$Cl catalyst incorporated into multi-walled carbon nanotubes (MWCNT) was developed. Current densities of ~ 4 mA/cm^2 and selectivities (FE_{CO}) of 99% were achieved at -0.56 V vs. RHE in CO_2 saturated aqueous $KHCO_3$ solutions. Supporting Re(tBu-bpy)$(CO)_3$Cl on MWCNTs significantly increases current densities, decreases overpotential, retains high selectivity for reduction of CO_2 to CO, and allows operation in water at pH = 7.3 compared to the molecular catalyst in acetonitrile solution. The Re/MWCNT electrocatalysts achieve TON > 5600 and TOF > 1.6 s^{-1}. A simple approach is described below for preparation of selective and robust hybrid electrodes by incorporation of the Re catalyst into the structure of highly porous heterogeneous materials. These electrodes can easily be scaled up to desired manufacturing dimensions due to their robust nature and simplicity of preparation.

2.2 Preparation and characterization of Re(tBu-bpy)/MWCNT electrodes

Re(4,4'-tBu-2,2'-bpy)$(CO)_3Cl$ was synthesized according to a previously published procedure.[14] The Re(tBu-bpy)/MWCNT electrodes were prepared by drop casting a solution of Re(tBu-bpy)$(CO)_3Cl$ and MWCNT : Carbon Nanofiber (CNF) (5 : 2) onto Tokai glassy carbon electrode and dried at 150 ^{o}C for 1 hour prior to CV experiments. Detailed preparation steps are described in the Methods section below.

The modified electrodes were characterized with IR, NMR, XPS, TEM, STEM/EDS and reactivity of these electrodes was studied using cyclic voltammetry and controlled potential electrolysis. Gas adsorption measurements were performed to determine the nitrogen adsorption isotherms and pore sizes of MWCNT.

XPS. High-resolution XPS analysis performed before and after 1h Controlled Potential Electrolyis (CPE) experiments showed Re 4f, N 1s and Cl 2p peak (Figure 2.1) consistent with XPS data for similar systems reported previously.[12] The Re 4f spectrum consisted of sharp peaks Re $4f_{5/2}$ and $4f_{7/2}$ at 44.3 and 41.8 eV respectively, with full widths at half-maximum (fwhm) of 1.09, 1.09 eV respectively, indicating a homogeneous environment around the rhenium center (Figure 1a). No peaks were observed at 40.3, 42.7 eV expected for Re^0 nanoparticles.[15] The N 1s spectra consist of a single sharp peak at 400.29 eV (fwhm 0.98 eV) for the sample before CPE and slightly shifted N 1s peak at 400.35 eV (fwhm 0.98 eV) for the sample after 1 h CPE (Figure 1b). The Cl 2p peaks were detected at 198.0 eV for Cl $2p_{1/2}$ and 199.7 eV for Cl $2p_{3/2}$ (Figure 1c) for the sample before CPE and broader Cl 2 p peaks at 198.2 and 199.7 eV after CPE. XPS of blank Re(tBu-bpy)$(CO)_3Cl$ on GCE without MWCNT presence revealed Re 4 f peaks at 44.0 and 41.6 eV. The Cl 2p peaks were detected at 198.7 eV for Cl $2p_{1/2}$ and 200.3 eV Cl $2p_{3/2}$). The N 1s spectra consist of a single sharp peak at 400.19 eV (fwhm 0.98 eV). Survey XPS analysis

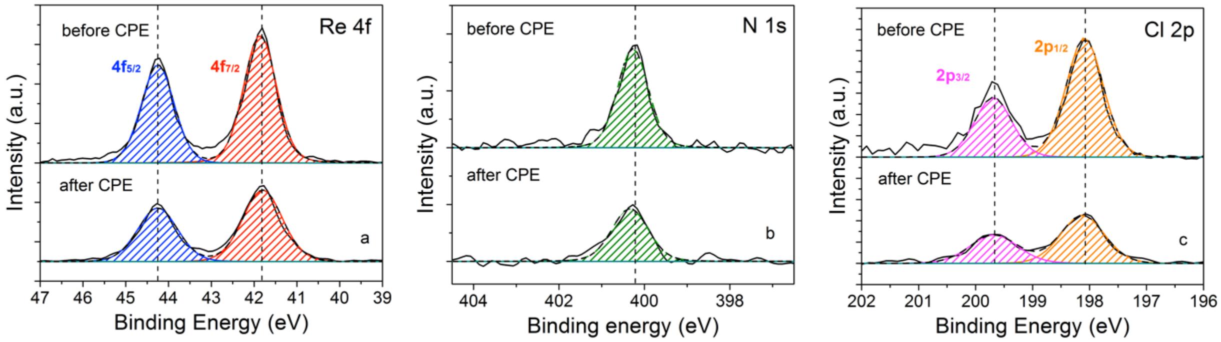

Figure 2.1 High-resolution XPS spectra for Re 4f (a), N 1s (b) and Cl 2p (c) of freshly prepared Re-tBu/MWCNT (top) and Re-tBu/MWCNT after 1h CPE experiments (bottom).

supports the structural composition of Re(tBu-bpy)$(CO)_3$Cl for freshly prepared samples and for samples measured after CPE experiments. For the freshly prepared samples the peak integrations reveal the atomic surface concentrations of 0.98 %, 1.93 % and 0.90 % for Re, N and Cl respectively, which integrates to 1 : 1.97: 0.92, consistent with expected Re/N/Cl ratio of 1 : 2 : 1 of Re(tBu-bpy)$(CO)_3$Cl.

For samples measured after CPE the atomic surface concentrations are 0.98 %, 1.96 % and 0.83 % for Re, N and Cl respectively, with Re/N/Cl ratio of 1 : 2 : 0.85, indicating a diminished Cl concentration, that can be explained by chloride dissociation reported for analogous systems.[12, 16] We note that only ca. 7.6 % of the Cl content of the samples is lost after CPE. This may indicate that a large fraction of Re(tBu-bpy)$(CO)_3$Cl sites are not responding to electrolysis, since the result of single electron reduction of the catalyst is known to be chloride dissociation.[14]

^{1}H NMR. To analyze the composition of electrodes after CPE samples were soaked in deuterated acetonitrile and analyzed via ^{1}H NMR spectroscopy. Chemical shifts corresponding to bipyridine ligand were detected and matched with the spectra of Re(tBu-bpy)$(CO)_3$Cl.[14] ^{1}H NMR (400 MHz, CD_3CN): δ 1.45 (s, 18H, tBu), 7.64 (dd, 2H), 8.41 (d, 2H), 8.88 (d, 2H).

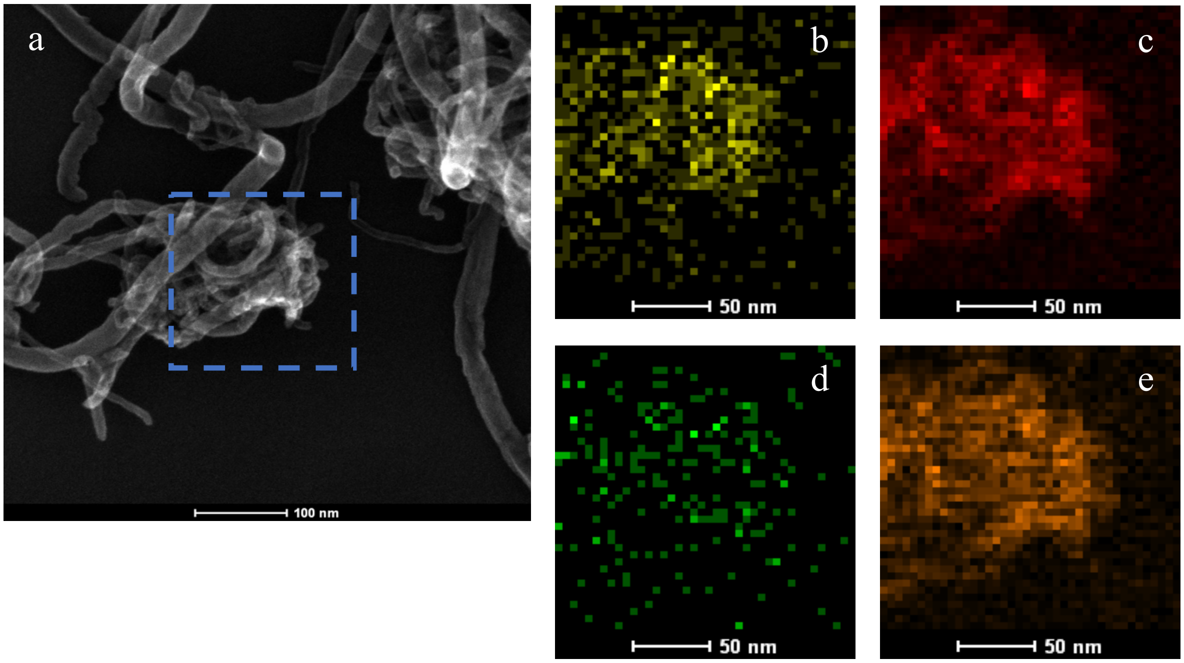

Figure 2.2 STEM image of Re-tBu/MWCNT material (a) and corresponding EDS maps of Re in yellow (b), of C in red (c), of Cl in green (d) and N in orange (e). Because the X-ray energies of C (0.277) and N (0.392) are very close their signals overlap.

Solution IR. The IR experiments of the electrodes soaked in MeCN showed IR peaks υ(CO) 2023, 1916, 1898 cm^{-1} and matched with the IR spectra of Re(tBu-bpy)(CO)$_3$Cl.

KBr pellet IR. A sample of Re(tBu-bpy)(CO)$_3$Cl of a known mass was pressed into a pellet with KBr salt and was analyzed using infrared spectroscopy. The IR spectra showed CO peaks at υ(CO) 2017, 1903, 1884 cm^{-1}. These pellets with four known concentrations were used

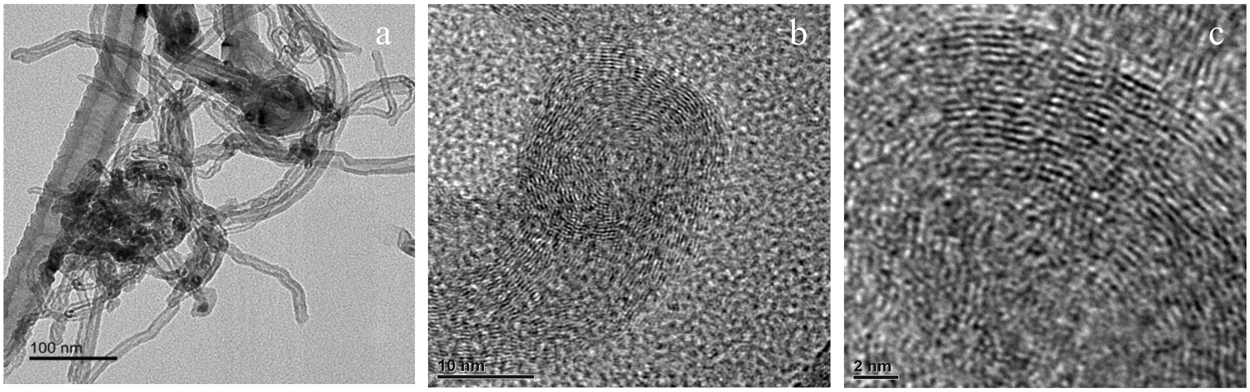

Figure 2.3 TEM images of Re(tBu-bpy)/MWCNT (electrode 3) at 100 kX (a) at 280 kX (b) and 690 kX magnification (c)

as a standard to plot a calibration line for the future measurements. The solid samples of Re(tBu-bpy)/MWCNT with various Re(tBu-bpy)$(CO)_3Cl$ loadings were pressed into KBr pellets to perform IR experiments of Re(tBu-bpy)$(CO)_3Cl$ adsorbed on MWCNTs. These samples were prepared by mixing electrode materials scraped from the electrode surface with a surgical blade with dry KBr salt. The IR spectra of these samples matched with a standard and showed three CO stretches at 2019, 1900, 1884 cm^{-1}. Thus, catalyst concentrations for three different Re(tBu-bpy)/MWCNT samples were calculated.

TEM/STEM-EDS. Transmission electron microscopy (TEM) was conducted to study the structural morphology of the electrodes. TEM revealed that Re(tBu-bpy)/MWCNT electrodes consist of hollow tubular nanotubes and conical nanofibers with the average diameter of ~15 nm for nanotubes and ~35 nm for nanofibers (Figure 2.3). The TEM at magnification of 100 kX showed MWCNTs aggregated around CNFs which add stability to the electrode material. The corresponding energy dispersive X-ray spectroscopy (EDS) maps showed that Re homogeneously distributed throughout the nanotube structures (Figure 2.2). The distribution of C and N elements match the nanotube structures and overlap due to close X-ray energies of C (0.277) and N (0.392). The EDS maps of Re and Cl show some response outside of the carbon nanotubes structures due to the instrumental noise that is typical at this magnification.

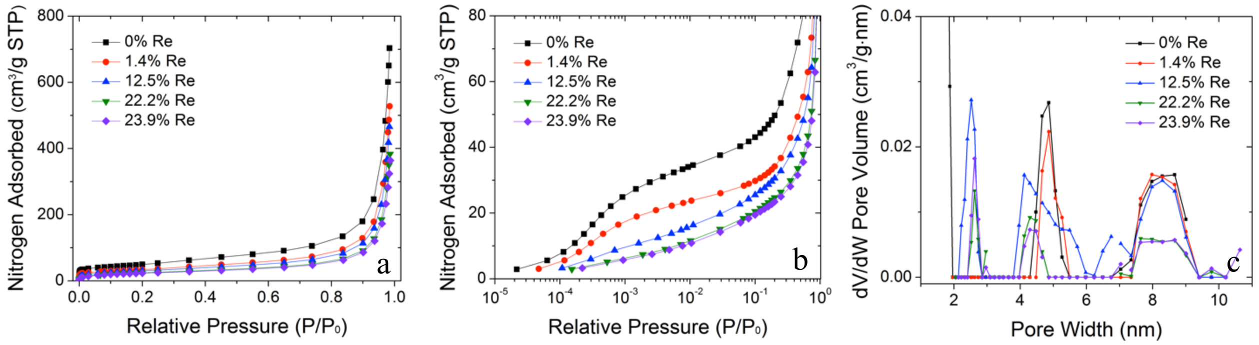

Figure 2.4 N_2 adsorption isotherms (77 K) of Re-loaded MWCNT/CNF composites in (**a**) linear and (**b**) log scale; (**c**) DFT pore size distributions of samples calculated from N_2 isotherms (77 K).

Gas adsorption measurements. Materials were characterized by N_2 physisorption at 77 K (Micromeritics ASAP 2020) after a 12 h activation under vacuum at 423 K (Figure 2.4 A, B). Brunauer-Emmet-Teller (BET) surface areas were calculated following established consistency criterion.[17] The composite sample without rhenium demonstrates a comparable surface area to other reported MWCNTs[18-22], although literature values vary greatly. Increasing loading of the rhenium complex results in surface area loss in excess of the added non-porous mass, indicating surface adsorption.

Sample pore size distributions (PSD) were calculated using the Microactive software package (Micromeritics) as multiwalled nanotubes under the DFT Pore Size model (Figure 2.4 C). The PSD of the blank sample shows a bimodal pore size distribution up to 10 nm—pore volume beyond this point is poorly defined and likely a result of interparticle condensation rather than intrinsic material porosity—which is closely mimicked by samples with low (1.4%) rhenium loading. Intermediate rhenium loadings (12.5%) result in noticeable changes in the PSD, where new pore distributions appear near 2.5 nm and 7 nm, likely from the disruption of the larger parent distributions. Moreover, the previously well-defined distribution at 5 nm is noticeably broadened. Further increasing (>20%) rhenium content continues to disrupt the pristine PSD, with a pronounced loss of cumulative porosity throughout the distribution. The changes in PSD in conjunction with the decreases in BET surface area suggest that the rhenium complex is located within the pores of the substrate, though it is not possible to rule out the presence of external complex adsorption.

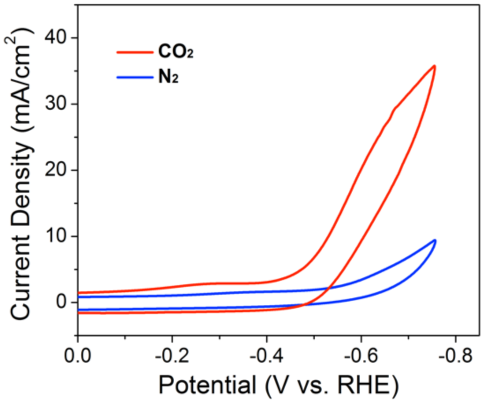

Figure 2.5 CV of Re(tBu-bpy)/MWCNT under N_2 (blue) and CO_2 (red) in 0.5 M $KHCO_3$ taken prior to CPE experiment. Electrode 4 was used as a working electrode, Ag/AgCl as a reference, Pt as a counter electrode. Scan rate 100 mV/s.

2.3 Electrochemistry

Cyclic voltammetry. The cyclic voltammetry (CV) experiments were performed using a three electrodes cell configuration, with platinum as a counter, Ag/AgCl as a reference and modified Re(tBu-bpy)/MWCNT as the working electrode at 100 mV/s. CV experiments were performed in 0.5 M $KHCO_3$ under N_2 or CO_2 atmosphere, unless stated otherwise. Electrodes with various Re(tBu-bpy) loadings were investigated trough CV and CPE experiments and the results are summarized in Table 2.1. A dramatic increase in current is observed when the applied potential reached -0.56 V vs. RHE under CO_2 in comparison to N_2 atmosphere (Figure 2.5). Current densities of 30 mA/cm^2 were achieved with electrodes containing 23.08 wt% of catalyst. The current density was found to decrease with decreasing catalyst loading and was less than 10 mA/cm^2 for electrode 1. Oversaturation of the carbon nanotube surface was found to occur when catalyst loading exceeded the concentration of 25 wt%, and this resulted in diminished current during CV and CPE experiments (Figure 2.6).

Table 2.1 Summary of electrocatalytic CO_2 reduction using Re(tBu-bpy)/MWCNT electrodes.

Electrode #	**Re(tBu-bpy) (wt %)**	**Charge (C)**	**[CO] (µmol)**	**FE (% CO)**	**FE (% H_2)**	**TOF (h^{-1})**	**TON_{EA} (CV)**	**TOF_{EA} (CV) (s^{-1})**	**I (mA/cm^2)**
1	0.42	3.7	16	83	15	297	2280	0.6	1.0
2	2.50	4.6	21	94	5	124	2703	0.8	1.3
3	13.9	11.1	57	99	1	38	5161	1.4	3.1
4	23.1	14.4	73	99	1	27	5619	1.6	4.0
5	25.2	7.6	33	99	1	12	4013	1.1	2.1

CPE experiments. The composition, quantity, and rate of the product formation was investigated via controlled potential electrolysis (CPE) experiments. CPEs were performed in a three-neck cell (V = 89 ml) at -0.56 V vs. RHE in 0.5 M $KHCO_3$ solution (35 - 40 ml) saturated with CO_2 gas. Under these conditions in the absence of the catalyst bare MWCNTs on a glassy carbon electrode produced H_2 with 100% Faradaic efficiency and very low current densities (0.18 mA/cm^2). When loaded with Re(tBu-bpy), these electrodes displayed high current densities which were found to be dependent on the catalyst loading. A current density of 1.0 mA/cm^2 was achieved with electrode **1** (0.42 wt% Re-tBu), 1.3 mA/cm^2 was achieved with electrode **2** (2.5 wt% Re-tBu), 3.1 mA/cm^2 with electrode **3** (13.9 wt% Re-tBu) and reached the maximum of 4.0 mA/cm^2 for electrode **4** (23.1 wt% Re-tBu) (Figure 2.6). A decline in current density was observed for electrode **5**, when catalyst loadings exceeded 25 wt% suggesting that these electrodes are susceptible to a blocking effect at higher catalyst loadings. This was somewhat surprising since a Re catalyst loading of 25 wt% corresponds approximately to one Re atom per

168 carbon atoms in the hybrid material. The headspace was analyzed via gas chromatography after 1 h of electrolysis and revealed Faradaic efficiency (FE) of 99% for CO and less than 1 % H_2 for the electrodes **3**, **4** and **5**. The selectivity for CO decreased when the catalyst loadings were decreased and corresponded to FE(CO) of 97 % for electrodes **7** and **8** and reached FE(CO) of 94 % for electrodes **2** and **6**. When the loading of the catalyst was decreased to 0.42 % (electrode **1**) the selectivity for CO decreased to 84 %. We further explored the performance of electrode **4** and carried out CPE experiments that proceeded for 7 hours at -0.56 V vs. RHE in 0.5 M $KHCO_3$ solution saturated with CO_2 gas. The headspace analysis via gas chromatography was performed every half an hour and revealed that the Faradaic efficiency of 99% for CO remained constant throughout the course of the experiment without deactivation of the catalyst (Figure 2.7). Furthermore, due to rapid CO formation and its low solubility in water, a profusion of CO bubbles was observed on the surface of the electrodes during CPE experiments.

2.4 Methods

Materials: Chemicals were purchased from Sigma Aldrich and Fisher Scientific and used without further purifications. Multi-walled carbon nanotubes (MWCNT) (>98% carbon basis, O.D. x L 6-13 nm x 2.5-20 μm) and graphitized carbon nanofiber (CNF) (iron-free, composed of conical platelets, D x L 100 nm x 20-200 μm) were purchased from Sigma Aldrich. Glassy carbon plates (SA-3, 100 x 100 x t3 mm) were purchased from Tokai Carbon and pre-cut to the area of 1 x 2 cm^2.

Preparation of glassy carbon electrodes. Tokai glassy carbon plates were polished with an alumina slurry (0.05 μm) with subsequent sonication in water, methanol and acetone. Polished glassy carbon plates were connected to a copper wire using an alligator clip and were covered with an epoxy so that the exposed working area of glassy carbon surface was equal to 1 x 1 cm^2.

Preparation and characterization of Re(tBu-bpy)/MWCNT electrodes. A solution of Re(tBu-bpy)(CO)$_3$Cl (2.6 mM, 0.7 ml, 1 mg, 13.9 wt%) in ethanol was added to 5 mg MWCNT and 2 mg CNF and sonicated for 5 minutes to disperse MWCNTs. DI water (0.3-0.5 ml) was added to the mixture to promote saturation and faster adsorption of Re(tBu-bpy)(CO)$_3$Cl by carbon nanotubes. The resulting yellow suspension was sonicated for 15 minutes until solution became colorless, which indicated of a complete adsorption of the catalyst by MWCNTs. This suspension was drop-casted onto a polished glassy carbon plate (1 x 1 cm^2) at 60^{o}C using a hot plate. Electrodes were dried in the oven for 1 hour at 150^{o}C prior to CV and CPE experiments. Electrodes made of drop-casted Re(tBu-bpy)-MWCNTs dissolved in a water/ethanol mixture tend to form more even surfaces without visible precipitate at the edges, these electrodes crack less frequently in comparison to the electrodes drop-casted from pure ethanol solutions. Sonication in pure ethanol solution without addition of water resulted only in partial adsorption of the catalyst by MWCNTs and therefore precipitation of catalyst agglomerates occurred at the edges of the electrode. When Re(tBu-bpy)(CO)$_3$Cl catalyst was directly drop-casted onto

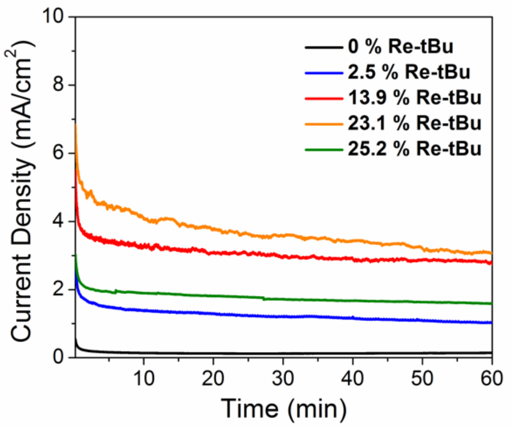

Figure 2.6 CPE experiments of Re(tBu-bpy)/MWCNT electrodes in CO$_2$ saturated 0.5 M KHCO$_3$ at -0.56 V vs. RHE.

MWCNTs, yellow agglomerates were seen at the surface of MWCNTs. These electrodes performed poorly in comparison to the electrodes prepared from sonicated Re(tBu-bpy)-MWCNTs ethanol/water solutions.

Electrochemistry. All cyclic voltammetry and controlled potential electrolysis (CPE) experiments were conducted using a Gamry Reference 600 potentiostat. A single compartment cell was used in all experiments with Re(tBu-bpy)/MWCNT/GCE as the working electrode (area 1 x 1 cm^2), A Pt wire spool was used as a counter electrode and Ag/AgCl as a reference electrode. Electrochemical CO_2 reduction experiments were performed on a Schlenk line using N_2 or CO_2 gas. Typically, a 0.5 M $KHCO_3$ solution in DI water was used as the supporting electrolyte. All experiments were conducted with the compensation for *iR* drop. CPE experiments were performed in a single compartment Gamry cell, with modified carbon electrodes as working, Ag/AgCl as reference and Pt wire spool separated from the working electrode with a glass frit as the counter electrode. Products were monitored using gas chromatograph (Hewlett-Packard 7890A) with a molsieve column and helium as carrier gas. Gas analysis was performed using 1 ml gas-tight syringe with the gas sample taken from the headspace of the CPE cell. All potentials were measured versus Ag/AgCl electrode and

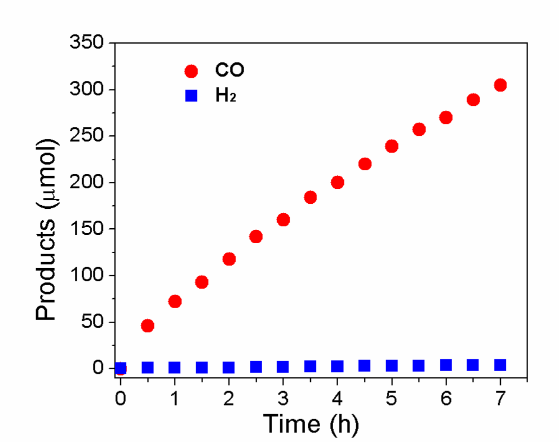

Figure 2.7 7 hours CPE experiment of Re(tBu-bpy)/MWCNT electrodes in CO_2 saturated 0.5 M $KHCO_3$ at -0.56 V vs. RHE.

converted to RHE according to the Nernst equation. Thus, the optimal operating potential of -0.56 V vs. RHE was determined as follows from cells employing Ag/AgCl reference electrodes:

$$E_{RHE} = E_{Ag/AgCl} + 0.059\ pH + E^0_{Ag/AgCl}$$

$$E_{RHE} = (-1.20) + 0.059 \times 7.23 + 0.209 = -0.56\ V$$

where E_{RHE} is the converted potential vs. RHE, $E_{Ag/AgCl}$ is the experimental potential measured against Ag/AgCl reference electrode, $E^0_{Ag/AgCl}$ vs. NHE is 209 mV (3 M NaCl) at 25°C.

The Re(tBu-bpy)/MWCNT electrodes displayed excellent activity and selectivity towards the electrochemical reduction of CO_2 to CO. These electrodes operated at -0.56 V vs. RHE in 0.5 M $KHCO_3$ with 99% selectivity for CO and only trace quantities of H_2.

The XPS survey analysis of Re(tBu-bpy)/MWCNT before and after CPE experiments revealed the presence of Re/N/Cl peaks consistent with the chemical composition of the Re(tBu-bpy)$(CO)_3$Cl complex. Samples analyzed before CPE experiments showed an integration ratio of Re/N/Cl peaks equal to 1/1.97/0.92, which is in agreement with the stoichiometry of Re(tBu-bpy)$(CO)_3$Cl. However, the integration of the same peaks in samples *after* CPE revealed a 7.6 % decrease in the Cl composition with overall Re/N/Cl ratio of 1/2/0.85. The diminished Cl peak can be explained by the chloride dissociation as discussed previously.[12] The dissociation of chloride is consistent with the mechanism for the homogeneous electrochemical reduction of CO_2 to CO by Re(t-Bu)$(CO)_3$Cl, where the dissociation of chloride is the initiation step in the catalytic cycle, providing a vacant site for CO_2 binding.[14, 23-25]

The observed high CO:H_2 selectivity of Re(tBu-bpy)/MWCNT electrodes is attributed to the high loadings of the Re(tBu-bpy) catalyst used in these experiments. At high concentration and surface coverage selectivity for CO corresponded to almost 100% and remained constant throughout 7 hours of CPE. High surface coverage by the Re catalyst appears to promote CO_2

reduction over native proton reduction that can occur at exposed carbon sites. When catalyst loadings were low (electrode **1**, 0.7 wt%) hydrogen production was observed to occur with Faradaic efficiency for H_2 = 15% and 84% for CO. When catalyst loadings were increased to 13.9 wt%, selectivity for H_2 decreased to < 1% with FE = 99 % for CO. To obtain maximum CO selectivity the Re(tBu-bpy) catalyst should be evenly dispersed onto the structure of MWCNTs to minimize carbon sites exposure that can be crucial for hydrogen suppression. Similar observations were made previously for Mn-catalyst/MWCNT and p-RuCP polymeric catalysts incorporated into CNTs and carbon cloth.[7, 26]

Control experiments under a nitrogen atmosphere showed production of H_2, and no CO was detected during CPE experiments. Bare MWCNT/GCE without Re(tBu-bpy) showed exclusive production of hydrogen with FE (H_2) = 100%. Electrodes without MWCNTs with only Re(tBu-bpy) directly drop casted on glassy carbon surface showed almost no electrochemical activity towards CO_2 reduction at the same conditions. Control CV experiments with CNF only showed no change in current under CO_2 in comparison to N_2 with very low CPE current and hydrogen production with 100% Faradaic efficiency.

The TOF frequencies measured during CPE experiments and calculated per total concentration of catalyst were found to range from 297 to 12 h^{-1}, depending on the catalyst loadings. It is important to note that the TOF values were calculated based on the *total* amount of Re(tBu-bpy) in the bulk material and are therefore the extreme lower limit of the actual catalyst TOF values that should be calculated based on the amount of *electroactive* catalyst.[27] The amount of electroactive catalyst can be obtained through integration of the area of a Re(tBu-bpy) CV. In acetonitrile Re(tBu-bpy)$(CO)_3Cl$ displays two one electron reductions that were previously assigned to a bipyridine-based reduction followed by a metal based $Re^{I/0}$ reduction.[25]

We were able to detect a Re(tBu-bpy) redox peak in 0.5 M $KHCO_3$ at a scan rate of 25 mV/s at -0.38 V vs. RHE, prior to the catalytic wave, for freshly prepared electrodes. We tentatively assign this feature to bipyridine ligand based redox process. Although, we noticed that the CV peak shifts after second scan and gets smaller after third scan and completely diminishes after 4-th scan. The fact that the intensity of the peak decreases and completely vanishes with consecutive scans may indicate strong electronic coupling between MWCNTs under bias and the Re catalyst. Similar phenomena were described previously for conjugated linkages in graphite-conjugated catalysts (GCC-Ru) electrodes, where a Faradaic current cannot be detected due to charge build up at the interface establishing an electric field gradient that changes the Fermi level of the electrode relative to the donor/acceptor states regardless of the applied potential. This eliminates the driving force for the outer-sphere electron transfer consistent with the double-layer theory for a molecule electronically coupled to the electrode.[28] The quantity of electroactive Re(tBu-bpy) for electrode **4** obtained by integration of the first peak area was calculated to be 1.3×10^{-8} mol. This compares to a value of 1.8×10^{-8} for CoPc-CN, and 2×10^{-9} for COF-367-Co.[6,27] Using our estimated value of electroactive Re in the Re(tBu-bpy)/MWCNT electrodes, we obtain $\mathrm{TON_{EA}} = 5619$ and $\mathrm{TOF_{EA}} = 1.6\ \mathrm{s^{-1}}$. The amount of electroactive catalyst was determined for all electrodes in the manner described here and was found to range from 1 - 8 % of the total catalyst loaded into the bulk electrode material. The amount of electroactive rhenium increased with increasing catalyst loadings until it reached a saturation level (electrode **5**) which is attributed to the formation of agglomerates of inactive catalyst and physical blocking of the electrode surface. Thus, the amount of EA Re for electrode **5** decreased, which was also reflected in lower current densities for this electrode. The $\mathrm{TOF_{EA}}$ values for all electrodes are summarized in Table 2.1. Although high surface coverage resulted in lower amounts of electroactive catalyst, the total coverage is necessary to suppress the competing hydrogen evolution reaction that occurs on the exposed sites of the carbon nanotubes.

A reasonable comparison was drawn between the performance of homogeneously catalyzed CO_2 reduction by Re(tBu-bpy)$(CO)_3Cl$ in acetonitrile and heterogeneous Re(tBu-bpy)$(CO)_3Cl$/MWCNT in water. The TOF for homogeneous CO_2 reduction by 1 mM Re(tBu-bpy)$(CO)_3Cl$ in acetonitrile in the presence of 3 M H_2O corresponds to TOF = 5 s^{-1} (average), with a maximum reported TOF of 16 s^{-1} for 10 M H_2O.[25] The maximum effective loading for heterogeneous Re(tBu-bpy)/MWCNT was 23 wt%, which at the operating conditions corresponds to 0.1 mM Re(tBu-bpy), loadings 10 times lower than that for homogeneous catalysis. It is worth noting that these electrodes operate in aqueous media where the solubility of CO_2 is almost 5 times lower than in acetonitrile.[29, 30] Furthermore, control CPE experiments in MeCN : 5% H_2O solution with 0.1 mM Re(tBu-bpy)$(CO)_3Cl$ and bare MWCNT/GCE exhibited hydrogen production with FE of 87 % and FE of 12 % for CO. This was attributed to the limited diffusion and mass transport of the catalyst to the highly porous surface of the MWCNT. When incorporated into the structure of the MWCNT catalyst material we obtain no such limitations because of the direct contact between the catalyst and the surface of the electrode.

Re(4,4′-tBu-bpy)$(CO)_3Cl$ is known for its catalytic activity for CO_2 reduction in organic solvents with the highest catalytic activity reported in acetonitrile in the presence of 1 M phenol as a proton source.[13] Without addition of Bronsted acids, but in the presence of advantageous water, the determined overpotential (η) is equal to 0.86 V, considering CO_2/CO equilibrium at -1.344 V vs. $Fc^{+/0}$.[31] Since in aqueous solutions CO_2/CO equilibrium corresponds to -0.11 V vs. RHE,[32] the reduction potential of -0.56 V vs. RHE is equal to the overpotential of 0.45 V for CO evolution, which is 0.41 V lower than η for the homogeneous Re catalyst in acetonitrile.

Previous studies showed that reactivity and selectivity of Re-bpy in organic solvents depends on the acid strength (pKa). The acidity of 0.1 M $KHCO_3$ solution saturated with CO_2 corresponds to pH = 6.81, and pH = 7.23 for 0.5 M $KHCO_3$.[33] However, for the Re(tBu-bpy)/MWCNT system a trade-off exists between acidity of the solution and mass transport of CO_2 to the active sites of the embedded catalyst. Thus, electrodes operated at -0.56 V vs. RHE in 0.1 M $KHCO_3$ performed poorly in comparison to 0.5 M $KHCO_3$ solution. The same behavior was reported for the CoPc/MWCNT system at -0.49 V vs. RHE[6] and was attributed to the decreased mass transport of CO_2 to the catalytic sites.[34]

It was found that the selectivity of the Re(tBu-bpy)/MWCNT depends on the applied potential. At -0.62 V vs. RHE the system still produces CO with Faradaic efficiency of 97% *vs.* 3% for H_2, but at -0.67 V vs. RHE, Faradaic efficiency decreased to 84 % for CO and 15% for H_2. Thus the Re(tBu-bpy)$(CO)_3$Cl/MWCNT electrodes display overpotentials for CO and H_2 evolution that favor CO evolution at less negative potentials than H_2 evolution, the reverse of normal thermodynamic expectations for these reactions.

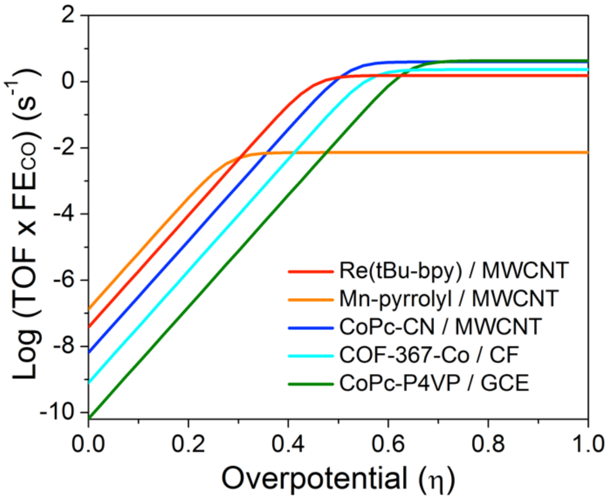

Figure 2.8 Catalytic Tafel plots for Re(tBu-bpy)/MWCNT (electrode 4) and other CO_2 reduction catalysts on MWCNTs, GCE or carbon fabric. CoPc-CN = cobalt-2,3,7,8,12,13,17, 18-octacyano-phthalocyanine, CoPc-P4VP = cobalt phthalocyanine poly-4-vinylpyridine at glassy carbon electrode at pH 4, COF-367-Co = cobalt porphyrin in piphenyl-4,4'-dicarboxaldehyde covalent organic framework on carbon fabric. Mn-MeCN = Mn(4,4′-di(1H-pyrrolyl-3-propyl carbonate)- 2,2′-bipyridine)$(CO)_3$MeCN]$^+$$(PF_6)^-$, Tafel plot for this catalyst was calculated based on the reported TON and bulk concentration of the catalyst, we assume that TON and TOF should be higher if calculated per electroactive species.

Developed Re(tBu-bpy)/MWCNT was compared to the best hybrid systems based on molecular catalysts on solid carbon supports. These data are summarized in Table 2.2. Although the highest current density, charge and TOF values were achieved with CoPc-CN in a flow reactor, Re(tBu-bpy)/MWCNT has lower operating potential and highest Faradaic efficiency for CO in comparison to other catalysts.

Table 2.2 Comparison of existing molecular electrocatalysts on various carbon supports

Catalyst	**Ecat. (V vs. RHE)**	**Current Density (mA/cm^2)**	**Charge (C)**	**TOF (s^{-1})**	**FE (CO)**
Re(tBu-bpy)	-0.56	4.0	14.4	1.6	99
Mn-pyrrolyl	-0.39	2.4	8.6	0.009	87
CoPc-CN	-0.63	15	54	4.1	98
CoPc-P4VP	-0.75	2.0	7.2	4.8	90
COF-367-Co	-0.67	2.9	10.4	2.6	90

Catalytic Tafel plots were created to benchmark our catalytic system with the existing molecular catalysts and they represent the relationship between thermodynamic and kinetic parameters: η and TOF. Tafel plots were calculated based on log TOF multiplied by FE(CO) and plotted against the corresponding overpotentials (Figure 2.8). Re(tBu-bpy)/MWCNT displayed the best optimal characteristics of η and TOF in comparison to other catalysts with overpotential of 0.45 and logTOF × FE(CO) = 0.2.

The Re(tBu-bpy)/MWCNT electrodes display exceptional electrocatalytic selectivity towards CO_2 reduction to CO. Re(tBu-bpy)/MWCNT electrodes are able to provide current densities of 4 mA/cm^2, with TON of 5620 and TOF of 1.6 s^{-1} at overpotential of 0.45 with selectivity of 99% for CO in water media. These electrodes require lower catalyst loadings than homogeneous CO_2 reduction with the same catalyst, exhibit remarkable selectivity towards CO_2 reduction over proton reduction due to high coverage of the electrode surface, and operate at pH 7.3 in aqueous solution. In conclusion, these electrodes operate at low overpotential with almost 100% selectivity for CO in aqueous media with high current densities, and overall performance far exceeding the molecular catalyst in homogeneous media.

The material for this chapter comes directly from a manuscript in preparation entitled "Re(tBu-bpy)$(CO)_3$Cl supported on multi-walled carbon nanotubes selectively reduces CO_2 in water" by Almagul Zhanaidarova, Brian Pimentel, Simon C. Jones and Clifford P. Kubiak,. The dissertation author is the primary author of this paper.

2.4 References

1. Tasis D.; Tagmatarchis N.; Bianco A.; Prato M., Chemistry of Carbon Nanotubes. *Chem. Rev.*, **2006**. *106*: p. 1105-1136.

2. Donck S.; Fize J.; Gravel E.; Doris E.; Artero V., Supramolecular assembly of cobaloxime on nanoring-coated carbon nanotubes: addressing the stability of the pyridine–cobalt linkage under hydrogen evolution turnover conditions. *Chem. Commun.*, **2016**. *52*: p. 11783-11786.

3. Tran P. D.; Le Goff A.; Heidkamp J.; Jousselme B.; Guillet N.; Palacin S.; Dau H.; Fontecave M.; Artero V., Bioinspired NanocatalystsDOI: 10.1002/anie.201005427Noncovalent Modification of Carbon Nanotubes with Pyrene-Functionalized Nickel Complexes: Carbon Monoxide TolerantCatalysts for Hydrogen Evolution and Uptake. *Angew Chem Int Ed Engl*, **2011**. *50*: p. 1371-1374.

4. Gentil S.; Lalaoui N.; Dutta A.; Nedellec Y.; Cosnier S.; Shaw W. J.; Artero V., Carbon-Nanotube-Supported Bio-InspiredNickel Catalystand ItsIntegrationinHybridHydrogen/AirFuelCells. *Angew Chem Int Ed Engl*, **2017**. *56*: p. 1845-1849.

5. Reuillard B.; Ly K. H.; Rosser T. E.; Kuehnel M. F.; Zebger I.; Reisner E., Tuning Product Selectivity for Aqueous CO2 Reduction with a Mn(bipyridine)-pyrene Catalyst Immobilized on a Carbon Nanotube Electrode. *J. Am. Chem. Soc.*, **2017**. *139*: p. 14425-14435.

6. Xing Zhang, Z.W., Xiao Zhang1, Liewu Li1, Yanyan Li, Haomin Xu, Xiaoxiao Li, Xiaolu Yu, Zisheng Zhang, Yongye Liang, Hailiang Wang, Highly selective and active CO2 reduction electrocatalysts based on cobalt phthalocyanine/carbon nanotube hybrid structures. *Nature Communiactions*, **2017**. *8*: p. 14675.

7. Shunsuke Sato, K.S., Keita Sekizawa, Satoshi Maeda, Takeshi Morikawa, Low-Energy Electrocatalytic CO2 Reduction in Water over Mn- + Complex Catalyst Electrode Aided by a Nanocarbon Support and K Cations. *ACS Catal.*, **2018**. *8*: p. 4452-4458.

8. Kyle A. Grice, C.P.K., Advances in Inorganic Chemistry. *Volume in CO2 Chemistry*, **2014**. *66*: p. 163-188.

9. O'Toole, T.R.S., B. P.; Bruce, M. R. M.; Margerum, L. D.; Murray, R. W.; Meyer, T. J., *J. Electroanal. Chem. Interfacial Electrochem.* , **1989**. *259*: p. 217-239.

10. Almagul Zhanaidarova, A.L.O., Christopher J. Miller, Simon C. Jones, and Clifford P. Kubiak, Selective Reduction of CO2 to CO by a Molecular Re(ethynyl-bpy)(CO)3Cl Catalyst and Attachment to Carbon Electrode Surfaces. *Organometallics*, **2018**.

11. Clark, M.L.R., B.; Ge, A.; Chabolla, S. A.; Machan, C. W.; Psciuk, B. T.; Song, J.; Canzi, G.; Lian, T.; Batista, V. S.; Kubiak, C. P. , *J. Phys. Chem. C* **2016**. *120*: p. 1657-1665.

12. Seokjoon Oh, J.R.G., Jeffrey T. Miller, Yogesh Surendranath, Graphite-Conjugated Rhenium Catalysts for Carbon Dioxide Reduction. *J. Am. Chem. Soc.*, **2016**. *138*: p. 1820-1823.

13. Melissa L. Clark, P.L.C., Martina Lessio, Emily A. Carter, Clifford P. Kubiak, *ACS Catal.*, **2018**. *8*: p. 2021−2029.

14. Jonathan M. Smieja, C.P.K., Re(bipy-tBu)(CO)3Cl−improved Catalytic Activity for Reduction of Carbon Dioxide: IR-Spectroelectrochemical and Mechanistic Studies. *Inorg. Chem.*, **2010**. *49*(20): p. 9283-9289.

15. Rabalais, Y.W., XPS, UPS, and TDS study of adsorption, oxidation, and hydrogenation of CO on rhenium. *Surface Science*, **1980**. *93*(2-3): p. 338-350.

16. Stor G. J.; Hartl F.; van Outersterp J. W. M.; Stufkens D. J., Spectroelectrochemical (IR, UV/Vis) Determination of the Reduction Pathways for a Series of [Re(CO)3(.alpha.-diimine)L']0/+ (L' = Halide, OTf-, THF, MeCN, n-PrCN, PPh3, P(OMe)3) Complexes. *Organometallics*, **1995**. *14*(3): p. 1115-1131.

17. Walton K. S.; Snurr R. Q., Applicability of the BET Method for Determining Surface Areas of Microporous Metal- Organic Frameworks. *J. Am. Chem. Soc.*, **2007**. *129*(27): p. 8552-8556.

18. Liu, B.L., Z.; Xu, S.; Han, D.; Lu, D.,, Enhanced Visible-Light Photocatalytic Activities of Ag3po4/Mwcnt Nanocomposites Fabricated by Facile in Situ Precipitation Method. *j. Alloys Compd.* , **2014**(596): p. 19-24.

19. Solhy, A.M., B. F.; Beausoleil, J.; Kihn, Y.; Gonçalves, F.; Pereira, M. F. R.; Órfão, J. J. M.; Figueiredo, J. L.; Faria, J. L.; Serp, P.,, Mwcnt Activation and Its Influence on the Catalytic Performance of Pt/Mwcnt Catalysts for Selective Hydrogenation. *Carbon*, **2008**(46): p. 1194-1207.

20. Yang, C.H., X.; Wang, D.; Dai, C.; Zhang, L.; Jin, H.; Agathopoulos, S.,, Ultrasonically Treated Multi-Walled Carbon Nanotubes (Mwcnts) as Ptru Catalyst Supports for Methanol Electrooxidation. *J. Power Sources*, **2006**. *160*: p. 187-193.

21. Kim, S.D.K., J. W.; Im, J. S.; Kim, Y. H.; Lee, Y. S.,, A Comparative Study on Properties of Multi-Walled Carbon Nanotubes (Mwcnts) Modified with Acids and Oxyfluorination. *J. Fluorine Chem.*, **2007**. *128*: p. 60-64.

22. Wang, W.S., P.; Kalck, P.; Silva, C. G.; Faria, J. L.,, Preparation and Characterization of Nanostructured Mwcnt-Tio2 Composite Materials for Photocatalytic Water Treatment Applications. *Materl. Res. Bull.*, **2008**. *43*(958-967).

23. Carter*†‡⊥, C.R.a.E.A., Influence of Weak Brønsted Acids on Electrocatalytic CO2 Reduction by Manganese and Rhenium Bipyridine Catalysts. *ACS Catal.*, **2015**. *5*(2): p. 900-908.

24. fac-Re(bpy)(CO)3Cl, E.o.t.S.o.P.-D.E.C.R.b., Elucidation of the Selectivity of Proton-Dependent Electrocatalytic CO2 Reduction by fac-Re(bpy)(CO)3Cl. *J. Am. Chem. Soc.* , **2013**. *135*(42): p. 15823-15829.

25. Smieja J. M.; Sampson M. D.; Grice K. A.; Benson E. E.; Froehlich J. D.; Kubiak C. P., Manganese as a Substitute for Rhenium in CO2 Reduction Catalysts:The Importance of Acids. *Inorg. Chem.* , **2013**. *52*: p. 2484-2491.

26. Arai T.; Sato S.; Morikawa T., A Monolithic Device for CO2 Photoreduction to Generate Liquid Organic Substances in a Single-Compartment Reactor. *Energy Environ. Sci.*, **2015**. *8*: p. 1998-2002.

27. Lin S., D.C.S., Zhang Y. B., Kornienko N., Nichols E. M., Zhao Y., Paris A. R., Kim D., Yang P., Yaghi O. M., Chang C. J.,, Covalent Organic Frameworks Comprising Cobalt Porphyrins for Catalytic CO2 Reduction in Water. *Science* **2015**. *349*(6253): p. 1208-1213.

28. Jackson M. N.; Oh S.; Kaminsky C. J.; Chu S. B.; Zhang G.; Miller J. T.; Surendranath Y., Strong Electronic Coupling of Molecular Sites to Graphitic Electrodes via Pyrazine Conjugation. *J. Am. Chem. Soc.*, **2018**. *140*(3): p. 1004-1010.

29. Wilhelm E.; Battino R.; Wilcock R. J., Low-Pressure Solubility of Gases in Liquid Water. . *Chem. Rev.*, **1977**. *77*(2): p. 219-262.

30. Smieja J. M., B.E.E., Kumar B., Grice K. A., Seu C. S., Miller A. J., Mayer J. M., Kubiak C. P., Kinetic and Structural Studies, Origins of Selectivity and Interfacial Charge Transfer in the Artificial Photosynthesis of CO. *Proc. Natl. Acad. Sci.*, **2012**. *109*: p. 15646-15650.

31. Iban Azcarate, C.C., Marc Robert, and Jean-Michel Savéant, Through-Space Charge Interaction Substituent Effects in Molecular Catalysis Leading to the Design of the Most Efficient Catalyst of CO2-to-CO Electrochemical Conversion. *J. Am. Chem. Soc.*, **2016**. *138*(51): p. 16639-16644.

32. Chen Y.; Li C. W.; Kanan M. W., Aqueous CO2 Reduction at Very Low Overpotential on Oxide-Derived Au Nanoparticles. *J. Am. Chem. Soc.*, **2012**. *134*: p. 19969-19972.

33. Chengzhen Chen, B.Z., Juhua Zhong Zhenmin Cheng, Selective electrochemical CO2 reduction over highly porous gold films. *J. Mater. Chem. A*, **2017**. *5*: p. 21955-21964.

34. Min X.; Kanan M. W., Pd-Catalyzed Electrohydrogenation of Carbon Dioxide to Formate: High Mass Activity at Low Overpotential and Identification of the Deactivation Pathway. *J. Am. Chem. Soc.*, **2015**. *137*(14): p. 4701-4708.

Chapter 3

Re(ethynyl-bpy) polymerized at glassy carbon electrodes

3.1 Introduction

This chapter describes earlier attempts to modify electrodes with Re(R-bpy) catalyst. The catalytic properties of Re(ethynyl-bpy)$(CO)_3Cl$ and Re(vinyl-bpy)$(CO)_3Cl$ were studied and compared with those of the previously reported Re(tBu-bpy))$CO)_3Cl$. As a molecular catalyst, Re(ethynyl-bpy)$(CO)_3Cl$ reduces CO_2 to CO with lower overpotential ($\eta \approx 0.525$ V), higher selectivity for CO (FE 96%), and higher reaction rate (I cat /I p = 27) compared to similar catalysts reported to date. The catalyst undergoes electropolymerization at the surface of a glassy carbon electrode in dry acetonitrile solution, creating a polymer film that is electroactive under a CO_2 atmosphere. In the presence of trifluoroethanol (TFE) (pKa 35.4, MeCN) these films exhibit high efficiencies for CO (FE CO 97%). On the basis of preliminary studies, these electrodes show promise as heterogeneous electrocatalysts. Further optimization and understanding of deactivation pathways will be required to make these systems practical. The ethynyl functionalized Re(ethynyl-bpy)$(CO)_3Cl$ catalyst also can be attached to graphitic carbon electrodes through the "click" reaction. This represents the first example of attachment of a CO_2 reduction catalyst to an electrode surface by "click" chemistry.

Re(tBu-bpy)$(CO)_3Cl$ is one of the most robust and effective homogeneous catalysts, and it is known for its high electrocatalytic activity to convert CO_2 to CO in the presence of weak Brønsted acids.[1] Functionalization of graphitic carbon electrodes with molecular catalysts of the Re(bpy)$(CO)_3Cl$ class are of great interest because these electrodes would require very low loadings of catalyst while providing heterogeneous systems, but with the activity and selectivity of a molecular catalyst. Surface modification of an electrode can proceed through either noncovalent interactions (adsorption) of an electroactive molecule on the surface[2, 3] or through covalent attachment of the molecule to the surface.[1, 4-6] Numerous strategies for surface modification of ferrocene on glassy carbon electrodes (GCEs) are available.[7-9] Despite this fact, there are only a few examples of covalent attachment of molecular catalysts to graphitic surfaces.[10, 11] Here, we describe on the catalytic properties of Re(ethynyl-bpy)$(CO)_3$Cl (complex 1) and Re(vinyl-bpy)$(CO)_3$Cl (complex 2) (Figure 3.1), as well as several surface attachment strategies in attempts to heterogenize complex 1 with the surface of a GCE.

Due to its high catalytic activity toward CO_2 reduction to CO and available triple bond Re(ethynyl-bpy) incorporation onto carbon surfaces is very appealing. New catalyst 1 that functions at lower potential and higher activity than most of its close counterparts was developed. The first attempts to modify carbon electrodes trough electropolymerization and "click" chemistry to design heterogeneous catalytic systems containing this catalyst were made. Further experiments are necessary to understand the effect of acids of various strengths and their conjugate bases on the product distributions and the stability of the polymer films as well as the properties of covalently modified electrodes under catalytic conditions. Despite the fact that Re(5-ethynyl-bpy)$(CO)_3$ Cl and similar ethynyl−bipyridine compounds were described

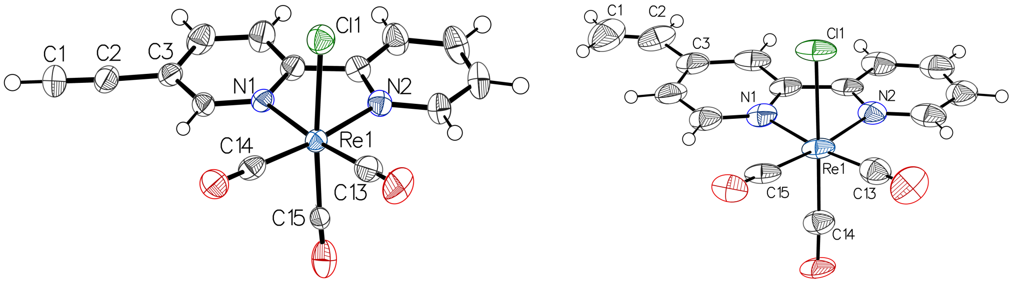

Figure 3. 1 Crystal structures of Re(ethynyl-bpy)$(CO)_3$Cl (1) and Re(vinyl-bpy)$(CO)_3$Cl (2). One of the two C1-C2 orientations is shown for complex 2. Thermal ellipsoids are shown at the 50% probability level.

previously, these compounds have never been studied for the electrochemical reduction of CO_2 to CO.[12, 13]

3.2 Synthesis and electrochemical properties.

Complexes 1 and 2 were prepared according to modified literature procedures and crystallographic data for 1 matched previously reported structural data.[12, 14]

Cyclic voltammetry experiments were carried out in dry MeCN with 0.1 M tetrabutylammonium hexafluorophosphate $TBAPF_6$ as the supporting electrolyte under nitrogen atmosphere. Complex 1 displays (i) a cathodic wave with reversible one-electron reduction at −1.56 V vs $Fc^{+/0}$, (ii) followed by a quasi-reversible reduction at −1.91 V vs $Fc^{+/0}$. These redox events were previously assigned to (i) a ligand-based reduction, (ii) succeeded by a metal-based reduction.[15] There is also an oxidative feature at +1.02 V vs $Fc^{+/0}$, that is assigned as an oxidation of the ethynyl substituent attached to the bipyridine ligand. In comparison, the CV of complex 2, the analogs of which were studied previously by Meyer's group,[16] revealed two one-electron reduction waves at −1.7 V vs Fc and −2.06 V vs $Fc^{+/0}$. The substantial difference in the reduction potentials of

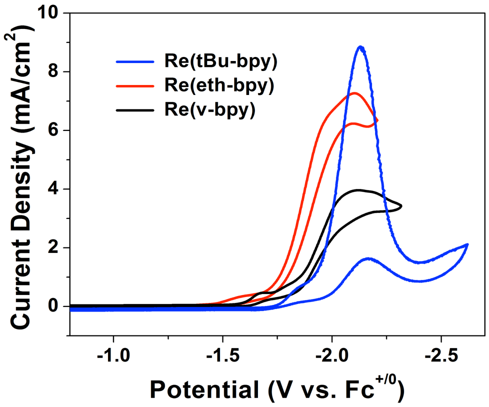

Figure 3.2 CV of complex 1, complex 2 and $Re(tBu\text{-}bpy)(CO)_3Cl$ under CO_2 with 1.5 M TFE in 0.1 M $TBAPF_6$/MeCN. Scan rate 0.1 V/s. The abbreviations eth = ethynyl and v = vinyl was used in the figure.

complex 1 can be explained by the difference of the Hammett parameter (σ_p) of the ethynyl and vinyl substituent. The ethynyl group is electron-withdrawing with a Hammett parameter of 0.23, whereas the vinyl substituent is electron-donating with a Hammett parameter of −0.04.[17] As the result, the electron-withdrawing substituted complex 1 has a reduction potential 140 mV less negative than complex 2 and 300 mV less negative than Re(tBu-bpy)$(CO)_3Cl$ ($\sigma_p = -0.2$).[1] We then compared the catalytic properties of complex 1 with complex 2 and Re(tBubpy)$(CO)_3Cl$ under the same catalytic conditions. The ratio of i_{cat}/i_p was used as the figure of merit to compare catalytic current responses, where i cat is the peak current under CO_2 and i_p is the current under inert conditions. The ratio i_{cat} /i_p is proportional to the catalytic rate constant, k cat.[18] CO_2 reduction studies of complex 1 (1 mM) were carried out in CO_2 saturated solution of 0.1 M $TBAPF_6$ /MeCN. The current enhancement was observed under CO_2 and i_{cat} /i_p value of 7 was determined. A large catalytic current increase was observed during the experiments of complex 1 with the addition of 1.5 M TFE as a proton source. The current increase initiates at −1.75 V vs Fc $^{+/0}$ and reaches a plateau at −2.1 V vs Fc $^{+/0}$ with i_{cat} /i_p value of 27. Product composition was investigated via controlled potential electrolysis (CPE) experiments at this potential and was monitored by gas chromatography. Analysis of the headspace after 1 h electrolysis revealed evolution of CO with Faradaic efficiency (FE) of 96% and less than 1 % of H_2. The current enhancement was observed for complex 2 under CO_2 with i_{cat}/i_p = 9. The current density remained unaffected by addition of TFE, and i_{cat} /i_p = 11 was determined in the presence of TFE. A value of i_{cat} /i_p = 30 was established for Re(tBu-bpy)$(CO)_3Cl$ with 1.5 M TFE in 0.1 M $TBAPF_6$ /MeCN and is in agreement with previously published data for this complex.[1, 19]

A comparison of the CVs of complex 1, complex 2, and Re(tBu-bpy)$(CO)_3Cl$ under CO_2 in the presence of 1.5 M TFE are depicted in Figure 3.2. A closer analysis of the CVs of these catalysts revealed the differences in the catalytic potential ($E_{cat/2}$), determined from the potential at half of the catalytic current.[20] The overpotential (η) was determined from the difference $E_{cat/2}$ - $E°_{CO2/CO}$ (CH_3CN).[1]

Determination of a catalytic rate constant k cat for complex 1 and Re(tBu-bpy)$(CO)_3$Cl was carried out under catalytic and inert conditions to identify intrinsic properties of the catalysts.

The k cat value was determined from the scan rate dependence studies according to Equation 3.1[18]

$$\frac{i_{\mathrm{cat}}}{i_{\mathrm{p}}} = \frac{1}{0.446}\sqrt{\frac{RT}{nF\upsilon}n'k_{\mathrm{cat}}} \qquad \text{Eq. 3.1}$$

Here F is Faraday's constant, R is the universal gas constant, T is the temperature, n is the number of unique electron transfer processes that occur at the electrode per catalyst (n = 2), n′ is the catalyst equivalents required per turnover (n′ = 1), υ is the scan rate, and k cat is the catalytic rate constant. TOF max was determined according to Equation 3.2[21]

$$\mathrm{TOF}_{\mathrm{max}} = k_{\mathrm{cat}} \qquad \text{Eq. 3.2}$$

The scan rate was increased until the current reached a plateau and k cat = 3100 s −1 was determined for complex 1. The k cat = 5000 s −1 was determined for the Re(tBu-bpy)$(CO)_3$Cl and is in agreement with the previously reported value.[1] A catalytic Tafel plot can be used to benchmark catalyst 1 with other reported catalysts. A Tafel plot illustrates the relationship between the thermodynamic (η) and kinetic (TOF) parameters of catalysts. The log TOF of catalyst 1 is comparable with log TOF of Re(tBu-bpy)$(CO)_3$Cl, but with 140 mV lower overpotential (η = 0.53). In fact, this overpotential is close to one of the lowest reported for the molecular electrocatalysts Mn(mes-bpy)$(CO)_3$Cl with η = 0.3 – 0.45 V, which show comparatively lower logTOFs.[22] The surprising relationship between less negative reduction potential and more active catalysis in 1 requires further study and theoretical explanation. However, in view of the remarkable properties of complex 1 as a catalyst, we have initiated an investigation of its attachment to electrode surfaces. The anchoring of homogeneous catalysts to solid supports through surface attachment can be a promising path to create robust, highly selective heterogeneous materials. Attempts to heterogenize Re(ethynyl-bpy)$(CO)_3Cl$ were made by polymerizing complex 1 at the surface of a glassy carbon electrode (GCE) and Tokai carbon electrode, creating a polymer film in a noncovalent fashion. When operated in saturated CO_2 solution with addition of 1.5 M TFE these electrodes exhibit exceptionally high current densities of 11 mA/cm^2. However, during subsequent scans current decrease was observed. CPE experiments carried at −2 V vs Fc $^{+/0}$ showed that in the presence of TFE these electrodes are able to reduce CO_2 to CO with 97% FE, however, the deactivation of these films was observed during the first minutes of electrolysis at these conditions. Electrolysis with acetic acid (pK a 23.5, MeCN) 1 exhibits stable current but with almost exclusive production of H_2 (FE 90%). Such an obvious dependence of product distribution and catalyst stability appears to depend on the strength of the conjugate base of these acids. Weaker Brønsted acids form stronger conjugate bases. TFE is a very weak acid (pK a 35.4, MeCN) 1 forms a stronger conjugate base that appears to deactivate the Re(ethynyl-bpy)$(CO)_3Cl$ film at the surface of the electrode. We have also attempted to use the pendent ethynyl group of 1 and the "click" reaction[23] to covalently attach it to the surface of a GCE. These electrodes show stable current responses in MeCN and in 0.5 M $KHCO_3$.

The material for this chapter comes directly from a manuscript entitled "Selective reduction of CO_2 to CO by a molecular Re(ethynyl-bpy)$(CO)_3Cl$ catalyst and attachment to carbon electrode surfaces" by Almagul Zhanaidarova, Andrew L. Ostericher, Chris J. Miller, Simon C. Jones S. and Clifford P. Kubiak, *Organometallics*, **2019**, *38* (6), pp 1204–1207. The dissertation author is the primary author of this paper.

3.3 References

1. Clark M.; Cheung P. L.; Lessio M.; Carter E. A.; Kubiak, C. P.,, Kinetic and mechanistic effects of bipyridine (bpy) substituent, labile ligand, and Bronsted acid on electrocatalytic CO_2 reduction by Re(bpy) complexes. *ACS Catalysis*, **2018**. *8*: p. 2021-2029.

2. Lydon B.R.; Germann A.; Yang J. Y., Chemical modification of gold electrodes via non-covalent interactions. *Inorg. Chem. Front.*, **2016**. *3*: p. 836-841.

3. Paulson S.; Morris K.; Sullivan P. B., A general preparative route to self-assembled monolayer surfaces of polypiridine ligands and their metal complexes. *J. Chem. Soc., Chem. Commun.*, **1992**. *21*: p. 1615-1617.

4. Hanna C.M.; Sanborn C. D.; Ardo S.; Yang J. Y., Interfacial Electron Transfer of Ferrocene Immobilized onto Indium Tin Oxide through Covalent and Noncovalent Interactions. *ACS Appl. Mater. Interfaces*, **2018**. *10*(15): p. 13211-13217.

5. Neri G.; Walsh J. J.; Wilson, C.; Reynal, A.; Lim, J. Y. C.; Li, X.; White, A. J.; Long, N. J.; Durrant, J. R.; Cowan, A. J, A functionalised nickel cyclam catalyst for CO_2 reduction: electrocatalysis, semiconductor surface immobilisation and light-driven electron transfer. *Phys. Chem. Chem. Phys.*, **2015**. *17*: p. 1562-1566.

6. Clark M.L.; Rudshteyn B.; Ge A.; Chabolla S. A.; Machan C. W.; Psciuk B. T.; Song J.; Canzi G.; Lian T.; Batista V. S.; Kubiak C. P.,, Orientation of Cyano-Substituted Bipyridine Re(I) facTricarbonyl Electrocatalysts Bound to Conducting Au Surfaces. *J. Phys. Chem. C*, **2016**. *120*(3): p. 1657-1665.

7. Devadoss A.; Chidsey C. E. D., Azide-Modified Graphitic Surfaces for Covalent Attachment of Alkyne-Terminated Molecules by “Click” Chemistry. *J. Am. Chem. Soc.*, **2007**. *129*(17): p. 5370-5371.

8. Sheridan M.V.; Lam K.; Geiger W. E., Covalent attachment of porphyrins and ferrocenes to electrode surfaces through direct anodic oxidation of terminal ethynyl groups. *Angew. Chem., Int. Ed.*, **2013**. *52*(49): p. 12897-12900.

9. Das A.K.; Engelhard M. H.; Liu F.; Bullock R. M.; Roberts J. A. S., The Electrode as Organolithium Reagent: Catalyst-Free Covalent Attachment of Electrochemically Active Species to an Azide- Terminated Glassy Carbon Electrode Surface. *Inorg. Chem. Front.* *52*: p. 13674-13684.

10. Jackson M.N.; Oh S.; Kaminsky C. J.; Chu S. B.; Zhang G.; Miller J. T.; Surendranath Y., Strong Electronic Coupling of Molecular Sites to Graphitic Electrodes via Pyrazine Conjugation. *J. Am. Chem. Soc.*, **2018**. *140*(3): p. 1004-1010.

11. Zhanaidarova A.; Moore C. E.; Gembicky M.; Kubiak C. P., Covalent attachment of [Ni(alkynyl-cyclam)]2+ catalysts to glassy carbon electrodes. *Chem. Commun.*, **2018**. *54*: p. 4116-4119.

12. Koutsantonis, G.A.; Low P. J.; Mackenzie C. F. R.; Skelton B. W.; Yufit D. S., Coordinating Tectons: Bimetallic Complexes from Bipyridyl Terminated Group 8 Alkynyl Complexes. *Organometallics*, **2014**. *33*: p. 4911-4922.

13. Mackenzie, C.F.R.; Bock S.; Lim C.-Y.; Skelton B. W.; Nervi C.; Wild D. A.; Low P. J.; Koutsantonis G. A., Coordinating Tectons. Experimental and Computational Infrared Data as Tools To Identify Conformational Isomers and Explore Electronic Structures of 4-Ethynyl-2,2′-bipyridine Complexes. *Organometallics*, **2017**. *36*(1946-1961).

14. Nie H.-J.; Yao J.; Zhong Y.-W., Synthesis of Vinyl-Substituted Polypyridyl Ligands through Suzuki Miyaura Cross-Coupling of Potassium Vinyltrifluoroborate with Bromopolypyridines. *J. Org. Chem.*, **2011**. *76*: p. 4771-4775.

15. Benson, E.E.; Grice K. A.; Smieja J. M.; Kubiak C. P., Structural and spectroscopic studies of reduced [Re(bpy-R)$(CO)_3$] species relevant to CO_2 reduction. *Polyhedron*, **2013**. *58*: p. 229-234.

16. O'Toole T.R.; Sullivan B. P.; Bruce M. R.-M.; Margerum L. D.; Murray R. W.; Meyer T. J., Electrocatalytic reduction of CO, by a complex of rhenium in thin polymeric films. *J. Electroanal. Chem. Interfacial Electrochem.*, **1989**. *259*(217-239).

17. Hansch C.; Leo A.; Taft R. W., A survey of Hammett substituent constants and resonance and field parameters. *Chem. Rev.*, **1991**. *91*(2): p. 165-195.

18. Costentin, C.; Saveant J. M., Multielectron, Multistep Molecular Catalysis of Electrochemical Reactions: Benchmarking of Homogeneous Catalysts. *ChemElectroChem*, **2014**. *1*(7): p. 1226-1236.

19. Smieja J.M.; Kubiak C. P., Re(bipy-tBu)$(CO)_3Cl$ − improved Catalytic Activity for Reduction of Carbon Dioxide: IR-Spectroelectrochemical and Mechanistic Studies. *Inorg. Chem.* , **2010**. *49*(20): p. 9283-9289.

20. Azcarate I.; Costentin C.; Robert M.; Saveant J. M., ThroughSpace Charge Interaction Substituent Effects in Molecular Catalysis Leading to the Design of the Most Efficient Catalyst of CO_2-to-CO Electrochemical Conversion. *J. Am. Chem. Soc.*, **2016**. *138*(5): p. 16639-16644.

21. Azcarate, I.C., C.; Robert, M.; Saveant, J. M.,, Dissection of Electronic Substituent Effects in MultielectronMultistep Molecular Catalysis. Electrochemical CO_2-to-CO Conversion Catalyzed by Iron Porphyrins. *J. Phys. Chem. C*, **2016**. *120*(15): p. 28951-28960.

22. Sampson M.D.; Kubiak C. P., Manganese Electrocatalysts with Bulky Bipyridine Ligands: Utilizing Lewis Acids To Promote Carbon Dioxide Reduction at Low Overpotentials. *J. Am. Chem. Soc.*, **2016**. *138*(4): p. 1386-1393.

23. Evrard D.; Lambert F.; Policar, C.; Balland, V.; Limoges, B.,, Electrochemical functionalization of carbon surfaces by aromatic azide or alkyne molecules: a versatile platform for click chemistry. *Chem. Eur. J.*, **2008**. *14*: p. 9286-9291.

Chapter 4

Electrografting of Ni-cyclam

4.1 Introduction

This chapter describes surface modification of glassy carbon electrodes (GCEs) with molecular electrocatalysts via direct anodic electrografting. Electrografting of [Ni(alkynyl-cyclam)]$^{2+}$ catalysts to the surface of GCEs in one simple step using inexpensive earth-abundant chemicals. When modified, these electrodes show reversible electrochemistry in organic solvents with zero peak-to-peak separations ($\Delta E = 0$) and non-diffusive I(V) profiles that are typical for heterogeneous redox materials. The Ni-catalyst/GCEs have the potential for significant scale up and applications in green energy production of carbon fuels from CO_2.

Surface modification of glassy carbon electrodes (GCEs) with molecular catalysts has been one of the most active and promising areas of electrocatalysis in the past decade. Surface modification of electrode materials through the covalent attachment of molecular catalysts is an essential step towards creation of new, scalable, robust electrocatalyst materials with unique structures and properties.[1] These materials can be used in basic electrochemical studies, energy conversion and storage, aerospace, biomedical and semiconductor industries.

Development of surface confined catalytic systems allows combining the most advantageous properties of homogeneous catalysis such as high reactivity and selectivity with those of heterogeneous catalysis - simple product separation, low catalyst loadings and simple catalyst regeneration. In homogeneous electrocatalysis, the diffusion of reactive species to the electrode surface is an important factor that affects the rate of catalysis. Electrodes with surface attached catalysts represent heterogeneous systems and are capable of increased catalytic rates due to the absence of catalyst diffusion limitations. There are only a few reports in the literature of surface modification of GCEs with molecular electrocatalysts, despite the fact that glassy carbon is one of the most common materials used in electrochemistry.

The successful covalent attachment of macrocyclic [Ni(alkynyl-cyclam)]$^{2+}$ electrocatalysts to the surface of GCE was developed. Despite high interest in its catalytic properties there are no previous reports in the literature of a covalent attachment of [Ni(cyclam)]$^{2+}$ to the surface of a GCE.

[Ni(cyclam)]$^{2+}$ is a low cost homogeneous electrocatalyst widely known for its high reactivity towards electrochemical reduction of CO_2 to CO at low potential (-1.2 V vs. NHE) and its ability to operate in aqueous media with high turnover rates and selectivity towards CO production at metal[2, 3] and glassy carbon electrodes[4]. Incorporation of a [Ni(cyclam)]$^{2+}$ catalyst to the electrode surface can significantly increase electrocatalytic rates and provide all of the benefits of heterogeneous catalysts. The recent report by Leem *et al.* describes a self-assembled Ni-cyclam-BTC on ITO glass and its enhanced electrocatalysis for water oxidation.[5] The incorporation of [Ni(cyclam)]$^{2+}$ into an artificial metalloenzyme described by Schneider *et al.* improved the selectivity of CO_2 reduction over hydrogen production by these enzymes.[6] In the paper by Neri and co-workers [Ni(cyclam-COOH)]$^{2+}$ was immobilized onto FTO surfaces for photoelectrochemical CO_2 reduction,[7] Kashiwagi *et al.* described polymer encapsulated [Ni(cyclam)]$^{2+}$ at a graphite felt electrode and showed that these modified electrodes can efficiently reduce various organic substrates.[8] Even though glassy carbon surface modification is challenging there are several techniques that allow efficient modification of electrode surfaces, including modification of electrodes through Click chemistry[9], hydrogen plasma treatment[10], electrochemical assisted attachment[11], etc. Anodic electrografting of ferrocenyl derivatives and porphyrins through ethynyl linkages to glassy carbon and other electrode surfaces was previously described by the Geiger group.[12] According to this method, the key step in the mechanism of anodic electrografting through terminal alkynes is the formation of alkynyl radicals. One-electron oxidation increases the acidity of the alkyne causing the loss of a proton and formation of alkynyl radicals which react with the surface of a GCE. Following this method, we successfully modified GCEs through the alkynyl radical electrografting procedure with [Ni(alkynyl-cyclam)]$^{2+}$ molecules. Newly modified electrodes were studied using electrochemical methods such as cyclic voltammetry (CV), scan rate dependence, and differential pulse voltammetry (DPV). The linear dependence of peak current versus scan rate confirmed the heterogeneous nature of surface bound redox species.

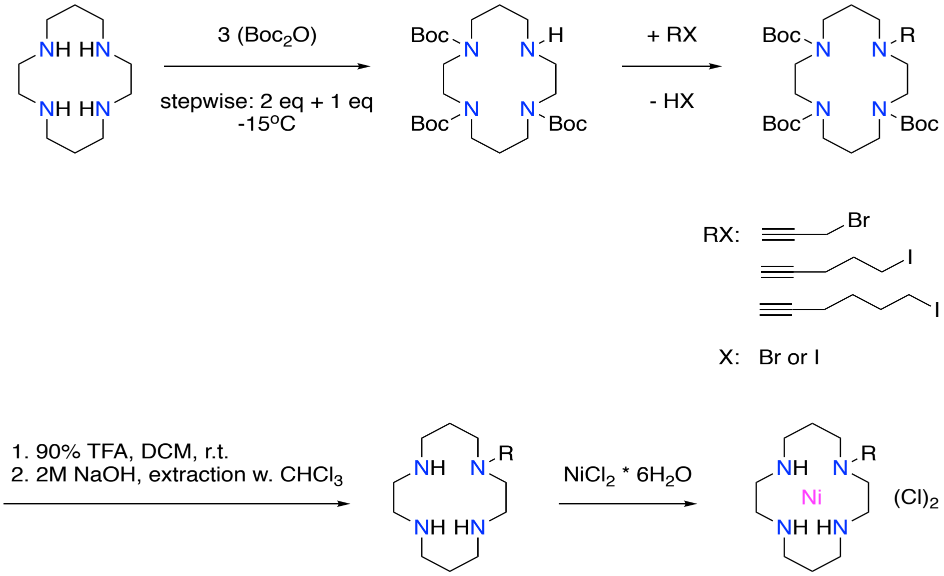

Scheme 4.1 Synthesis of [Ni(alkynyl-cyclam)]$^{2+}$ complexes.

4.2 Synthesis of alkynyl-cyclams and electrografting to GCE

The synthesis of new alkynyl-cyclam ligands as well as new nickel complexes [Ni-propargyl-cyclam]$^{2+}$ (**1**), [Ni-pentynyl-cyclam]$^{2+}$ (**2**) and [Ni-hexynyl-cyclam]$^{2+}$ (**3**) are described here. The synthetic route for alkynyl-cyclams includes following steps: selective triBoc-protection of cyclam, N-functionalization using propargyl bromide, 5-iodo-1-pentyne or 6-iodo-1-hexyne, deprotection in TFA/DCM solution, which resulted in the formation of a trifluoroacetate salt.[13, 14] The salt was basified with 2 M NaOH and the ligand was extracted with chloroform[15] (Scheme 1). The corresponding nickel complexes were obtained using the newly synthesized ligands and nickel chloride hexahydrate ($NiCl_2 \cdot 6H_2O$). A color change from green to purple was observed upon ligand coordination in anhydrous ethanol. Purple crystals suitable for the X-ray analysis were obtained through vapor diffusion in DCM/pentane. Crystal structures for [Ni(propargyl-cyclam)]$^{2+}$ (complex **1**), [Ni(pentynyl-cyclam)]$^{2+}$ (complex **2**) and Ni(hexynyl-cyclam)]$^{2+}$ (complex **3)** are shown in Figure 4.1.

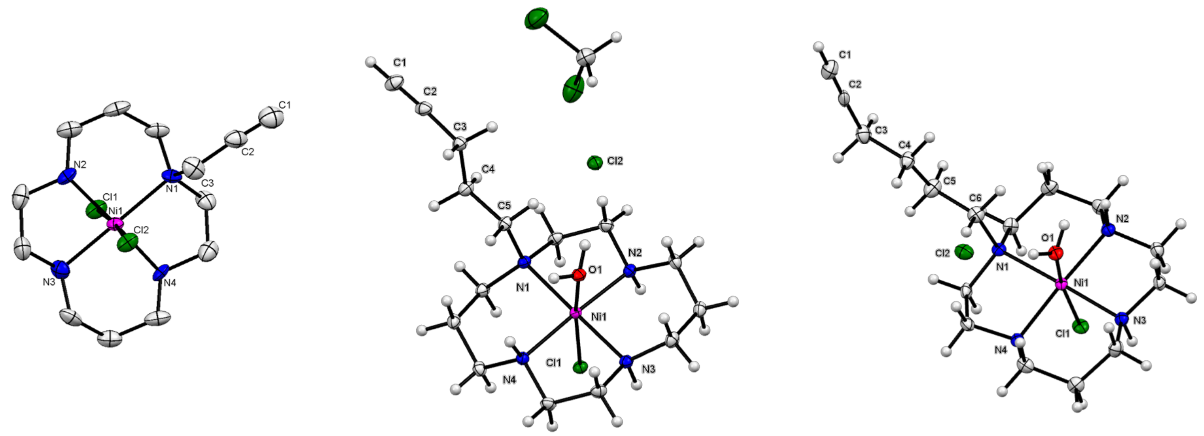

Figure 4.1 X-ray structures of complex **1**, **2** and **3**.

Homogeneous electrochemical CO_2 reduction experiments using the [Ni(alkynyl-cyclam)]$^{2+}$ complexes showed reactivity towards CO_2 reduction in MeCN/water mixtures and are good candidates for further development of a heterogeneous system with attached Ni(alkynyl-cyclam) complexes.

Homogeneous CO_2 reduction by [Ni(hexynyl-cyclam)]$^{2+}$ in acetonitrile/water mixture showed catalytic current enhancement at -1.65 V vs. Fc$^{+/0}$ at a glassy carbon electrode under CO_2 atmosphere (Figure S2). Notably, the reduction potential is almost 0.2 V less negative for complex **3** in comparison to a catalyst [Ni-cyclam]$^{2+}$ at the same conditions.[16] The same current increase was detected for complex **1** and **2** in the presence of 20% water under CO_2 atmosphere.

Table 4.1 Theoretical and experimental surface coverage of glassy carbon electrodes modified with [Ni(alkynyl-cyclams)]$^{2+}$.

	mod-GCE-1	**mod-GCE-2**	**mod-GCE-3**
Diameter (d, Å)	8.13	10.36	11.23
Charge (uC)	1.54	1.02	0.88
Theor. (10^{-10} mol/cm^2)	2.53	1.62	1.28
Exp. (10^{-10} mol/cm^2)	2.25	1.46	1.28

Cyclic voltammetry of complex **1** (0.5 mM) in DCM/TBAPF$_6$ solution showed Ni$^{III/II}$ couple at +0.35 V vs. Fc$^{+/0}$ as well as propargyl oxidation at +1.65 V vs. Fc$^{+/0}$ (Figure 4.2A). Multiple scans (up to 10 anodic scans) through the alkynyl group resulted in the attachment of [Ni(propargyl-cyclam)]$^{2+}$ at the GCE surface, as determined by CV after thorough rinsing of the modified electrode in DCM and transferring the electrode into a pure electrolyte solution.

Electrodes modified with complex **1** (mod-GCE-1) were studied using cyclic voltammetry and differential pulse voltammetry experiments. The reversible Ni$^{III/II}$ redox couple was observed at -0.1 V vs. Fc$^{+/0}$ and the peak to peak separation ΔE$_{1/2}$ was nearly 0 V which indicates the heterogeneous nature of the surface attached species and the absence of diffusion limitations (Figure 4.2B). Scan rate dependence studies were performed on newly prepared electrodes and were taken within the scan rate range of 10 – 70 mV/s (Figure 4.2 C). The peak current of Ni$^{III/II}$ redox couple increased linearly with increasing scan rate. The linear fit is another confirmation of the heterogeneous nature of the surface bound [Ni(propargyl-cyclam)]$^{2+}$. Similar behavior was observed for the GCE modified with complex **2** (mod-GCE-2) and complex **3** (mod-GCE-3). The CV of a complex **2** showed a reversible Ni$^{III/II}$ couple at +0.38 V vs. Fc$^{+/0}$ and the pentynyl

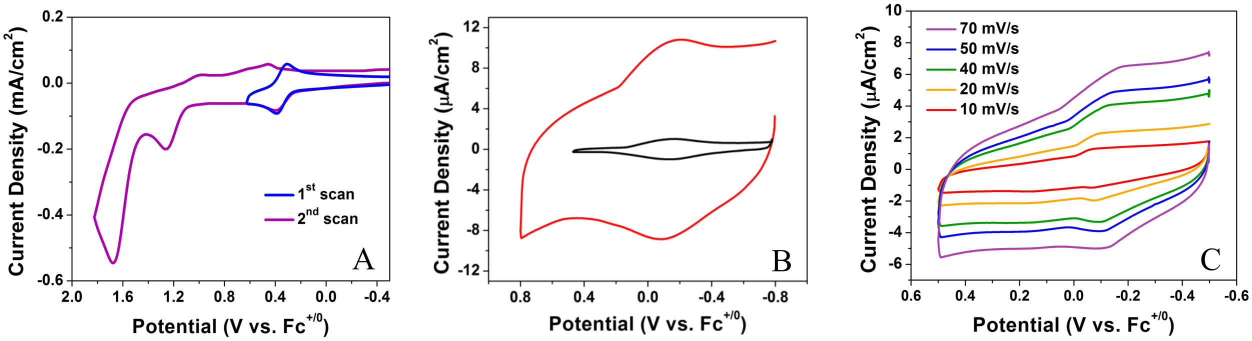

Figure 4.2 CV of [Ni(propagyl-cyclam)]$^{2+}$ in 0.1 M TBAPF$_6$ /DCM solution. Scan rate 100 mV/s (A). CV of mod-GCE-1 in 0.1 M TBAPF$_6$ in DCM. Scan rate 100 mV/s (red), 5 mV/s (black) (B). CV of mod-GCE-1 in 0.1 M TBAPF$_6$ in DCM at various scan rates (C).

oxidation peak at +1.93 V vs. $Fc^{+/0}$. After 10 scans mod-GCE-2 showed a reversible $Ni^{III/II}$ peak at -0.04 V vs. $Fc^{+/0}$ and the scan rate studies showed a linear dependence of peak current vs. scan rate. Cyclic voltammetry of complex **3** in 0.1M $TBAPF_6$ /DCM solution showed $Ni^{III/II}$ redox couple at +0.35 V vs. $Fc^{+/0}$ and the hexynyl oxidation at +1.8 V vs. $Fc^{+/0}$. GCE modified with **3** showed reversible $Ni^{III/II}$ redox couple at -0.03 V vs. $Fc^{+/0}$ with minimal $\Delta E_{1/2}$ in pure $TBAPF_6$/DCM solution. The peak current increased linearly with increasing scan rate similar to the scan rate dependence of mod-GCE-1. The redox potential difference (ΔE) between surface attached species and homogeneous species in solution decreased with the increasing length of a carbon chain linker.

Experimental surface coverages were obtained from the differential pulse voltammetry (DPV) and are based on the electrochemical charge (Q) passed through the surface of the electrode. Determination of the surface coverage of modified electrodes was calculated using Equation 4.1[17]:

$$\mathbf{\Gamma = Q/nFA} \qquad \text{Eq. 4.1}$$

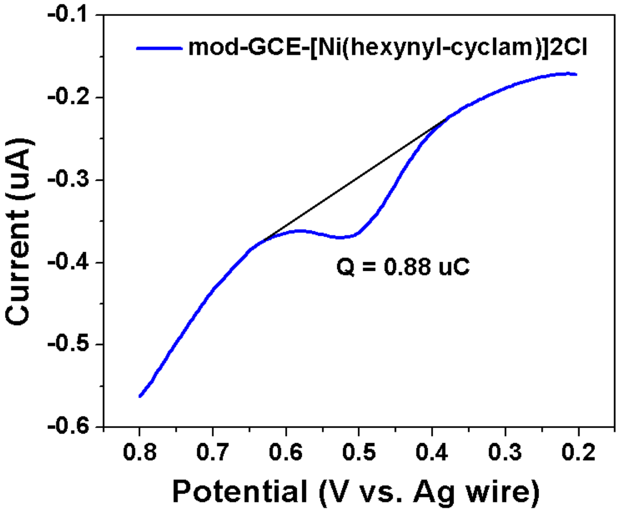

Figure 4.3 DPV experiment of mod-GCE-3 in 0.1 M TBAPF$_6$/DCM.

where n – number of electrons, F – Faradaic constant, A – the electrode surface area, Γ – the surface coverage in moles of adsorbed molecules per cm^2.

DPV experiments for the electrode modified with [Ni(hexynyl-cyclam)]$^{2+}$ showed a charge of 0.88 uC that corresponds to the surface coverage of 1.28x10^{-10} mol/cm^2 and is in exact agreement with theoretical value of 1.28 x 10^{-10} mol/cm^2 (Figure 4.3). The monolayer coverage was determined in all three cases. Theoretical and experimental surface coverages for all modified GC electrodes are summarized in Table 4.1.

Heterogeneous CO_2 reduction experiments using newly modified GCEs were carried out in 0.1 M TBAPF$_6$/MeCN solution with 20% water as a proton source. The CV shows a current increase at -1.45 V vs. Fc$^{+/0}$ under CO_2 and reached a plateau at -2.3 V vs. Fc$^{+/0}$.

Modification of GCEs with larger surface areas need to be prepared in order to carry out controlled potential electrolysis and identify products of CO_2 reduction by these electrodes.

The surface of the GCE was modified with [Ni(alkynyl-cyclam)]$^{2+}$ catalysts using direct anodic electrografting. Electrochemical studies performed on these electrodes showed that [Ni(alkynyl-cyclam)]$^{2+}$ molecules attached to the surface in heterogeneous fashion, eliminating diffusion limitations that are typical for homogeneous catalysis. CO_2 studies with [Ni(alkynyl-cyclam)]$^{2+}$ modified electrodes showed a current increase under CO_2 atmosphere in comparison to N_2. Further development of these catalytic systems at larger electrode surfaces can lead to efficient, selective and robust materials for the electrochemical reduction of CO_2 to energy-dense carbon products.

The material for this chapter comes directly from a manuscript entitled "Covalent attachment of [Ni(alkynyl-cyclam)]$^{2+}$ catalysts to glassy carbon electrodes" by Almagul Zhanaidarova, Curtis E. Moore, Milan Gembicky and Clifford P. Kubiak, Chem. Commun., 2018, 54, 4116 – 4119. The dissertation author is the primary author of this paper.

4.3 References:

1. Belanger D.; Pinson J., Electrografting: a powerful method for surface modification. *Chem. Soc. Rev.*, **2011**. *40*(7): p. 3995-4048.

2. Beley M.; Collin J. P.; Ruppert R.; Sauvage J. P., Electrocatalytic reduction of carbon dioxide by nickel cyclam in water: study of the factors affecting the efficiency and the selectivity of the process. *J. Am. Chem. Soc.*, **1986**. *108*(24): p. 7461-7467.

3. Wu Y.; Rudshtein B.; Zhanaidarova A.; Froehlich J. D.; Ding W.; Kubiak C. P.; Batista V. S., Electrode-Ligand Interactions Dramatically Enhance CO_2 Conversion to CO by the $[Ni(cyclam)](PF_6)_2$ Catalyst. *ACS Catal.*, **2017**. *7*(8): p. 5282-5288.

4. Froehlich J. D.; Kubiak C. P., The Homogeneous Reduction of CO_2 by [Ni(cyclam)]$^+$: Increased Catalytic Rates with the Addition of a CO Scavenger. *J. Am. Chem. Soc.*, **2015**. *137*(10): p. 3565-3573.

5. Leem Y. J.; Cho K.; Oh K. H.; Han S. H.; Nam K. M.; Chang J., A self-assembled Ni(cyclam)-BTC network on ITO for an oxygen evolution catalyst in alkaline solution. *Chem. Commun.*, **2017**. *53*: p. 3454-3457.

6. Shneider C. R.; Shafaat H. S., An internal electron reservoir enhances catalytic CO_2 reduction by a semisynthetic enzyme. *Chem. Commun.*, **2016**. *52*: p. 9889-9892.

7. Neri G.; Walsh J. J.; Wilson C.; Reynal A.; Lim J. Y. C.; Li X.; White A. J.; Long N. J.; Durrant J. R.; Cowan A. J., A functionalised nickel cyclam catalyst for CO_2 reduction: electrocatalysis, semiconductor surface immobilisation and light-driven electron transfer. *Phys. Chem. Chem. Phys.*, **2015**. *17*: p. 1562-1566.

8. Kashiwagi Y.; Kikuchi C.; Kurashima F.; Anzai J., Electrocatalytic reduction of aldehydes and ketones on nickel(II) tetraazamacrocyclic complex-modified graphite felt electrode. *j. Organomet. Chem.*, **2002**. *662*(1-2): p. 9-13.

9. Devadoss A.; Chidsey C. E. D., Azide-Modified Graphitic Surfaces for Covalent Attachment of Alkyne-Terminated Molecules by “Click” Chemistry. *J. Am. Chem. Soc.*, **2007**. *129*(17): p. 5370-5371.

10. DeClements R.; Swain G. M., Electrochemical and Surface Structural Characterization of Hydrogen Plasma Treated Glassy Carbon Electrodes. *Langmuir*, **1996**. *12*(26): p. 6578-6586.

11. Koefoed L.; Pedersen S. U.; Daasbjerg K., Covalent Modification of Glassy Carbon Surfaces by Electrochemical Grafting of Aryl Iodides. *Langmuir*, **2017**. *33*(13): p. 3217-3222.

12. Sheridan M. V.; Lam K.; Geiger W. E., Covalent attachment of porphyrins and ferrocenes to electrode surfaces through direct anodic oxidation of terminal ethynyl groups. *Angew. Chem. Int. Ed.*, **2013**. *52*(49): p. 12897-12900.

13. Fabbrizzi L.; Foti F.; Licchelli M.; Maccarini P. M.; Sacchi D.; Zema M., Light-Emitting Molecular Machines: pH-Induced Intramolecular Motions in a Fluorescent Nickel(II) Scorpionate Complex. *Chem. - Eur. J.*, **2002**. *8*(21): p. 4965-4972.

14. Tamanini E.; Katewa A.; Sedger L. M.; Todd M. H.; Watkinson M., A synthetically simple, click-generated cyclam-based zinc(II) sensor. *Inorg. Chem.*, **2009**. *48*: p. 322-324.

15. Yu M.; Price J. R.; Jensen P.; Lovitt C. J.; Shelper T.; Duffy S.; Windus L. C.; Avery V. M.; Rutledge P. J.; Todd M. H., P. J.; Todd M. H., Copper, Nickel, and Zinc Cyclam–Amino Acid and Cyclam–Peptide Complexes May Be Synthesized with "Click" Chemistry and Are Noncytotoxic. *Inrog. Chem.*, **2011**. *50*(24): p. 12823-12835.

16. Froehlich J. D.; Kubiak C. P., Homogeneous CO_2 Reduction by Ni(cyclam) at a Glassy Carbon Electrode. *Inorg. Chem.*, **2012**. *51*(7): p. 3932-3934.

17. Seo K.; Jeon I. C.; Yoo D. J., Electrochemical Characteristics of Ferrocenecarboxylate-Coupled Aminoundecylthiol Self-Assembled Monolayers. *Langmuir*, **2004**. *20*(10): p. 4147-4154.

Chapter 5

Future outlook.

Energy generated by renewable sources, like solar, wind and hydropower, provide electricity without giving rise to carbon emissions. Production of liquid fuels and chemicals using renewable sources of energy at an economically feasible cost should be a major effort of the future energy research. This includes development of batteries and energy storage sector as well as further development of the catalytic systems that would efficiently convert CO_2.

The current state of already developed oil and gas industries makes it very hard to compete with for at least next 50 years, when the prices for oil and gas are still relatively low. Sadly, CO_2 emissions and rising temperatures will continue to take place. The technologies that help to reduce CO_2 concentration in the atmosphere should be developed to help mitigate the consequences of continuous burning of fossil fuels.

5.1 The future of surface modification using molecular catalyst supported by MWCNTs.

The electrodes modification method that was described in Chapter 2 of this thesis has high potential to be applied to other molecular catalysts. The main drawback of this method is that only the small percentage of the bulk catalyst material appear to be electrochemically active. We now know that when the concentration of the catalyst on the surface of the MWCNTs exceeds curtain limit, the current efficiency drops down which is attributed to the blocking effect of the electrode surface. The future developments of this method should be focused on the even distribution of the catalyst throughout the surface of the carbon nanotubes, which can potentially increase turnover frequency of the catalyst.[1]

With the estimated average concentration of 1 ppb in the Erath's crust, rhenium metal considered to be one of the rarest elements on the planet with the average price of $1290 per pound in 2019. Many other molecular systems that contain abundant first row transition metals such as Mn, Ni, Fe, Co, Cu[2] can be explored for the electrodes modification using method that was developed in Chapter 2.

5.2 Building a device for the interstellar missions.

This research was supported by NASA/JPL with the initial idea to build an alternative device for the Mars Oxygen In-Situ Resource Utilization Experiment better known as MOXIE, that reduces CO_2 to CO and O_2 using yttria-stabilized zirconia and operates at 700°C.[3] The in-situ resource utilization provides a viable pathway to production of fuels and oxygen by reducing CO_2 from Martian atmosphere. The device that operates at room temperatures and less energy consuming would be an alternative for MOXIE.

The electrodes that were developed and described in Chapter 2 are currently being tested for an alternative device to MOXIE to reduce CO_2 to CO at the cathode and to produce O_2 gas at the anode.

5.3 References:

1. Zhang X.; Wu Z.; Zhang X.; Li L.; Li Y.; Xu H.; Li X.; Yu X.; Zhang Z.; Liang Y.; Wang H., Highly selective and active CO_2 reduction electrocatalysts based on cobalt phthalocyanine/carbon nanotube hybrid structures. *Nature Communications*, **2017**. *8*: p. 14675.

2. Smieja, J.; Sampson M. D.; Grice, K. A.; Benson, E. E.; Froehlich, J. D.; Kubiak, C. P.,, Manganese as a Substitute for Rhenium in CO_2 Reduction Catalysts: The Importance of Acids. *Inorganic Chemistry*, **2013**. *52*(5): p. 2484-2491.

3. West W., Addressing the Mars ISRU Challenge: Production of Oxygen and Fuel from CO_2 Using Sunlight. *Keck Institute for Space Studies* **2018**.